DEVELOPMENT AND APPLICATION OF A MODULAR WATERSHED-SCALE HYDROLOGIC MODEL USING THE OBJECT MODELING SYSTEM: RUNOFF RESPONSE EVALUATION

J. C. Ascough II, O. David, P. Krause, G. C. Heathman, S. Kralisch, M. Larose, L. R. Ahuja, H. Kipka

ABSTRACT. *This study reports on the integration of the J2K model (an object-oriented, hydrological system for fully distributed simulation of the water balance in large watersheds) under the Object Modeling System (OMS) environmental modeling framework and subsequent evaluation of OMS-J2K performance in the Cedar Creek watershed (CCW) in northeastern Indiana. The CCW is one of 14 benchmark watersheds in the USDA-ARS Conservation Effects Assessment Project (CEAP) watershed assessment study. Two input parameter sets were developed for OMS-J2K evaluation: (1) a "base parameter set" with parameter values taken from previous simulation studies where J2K was applied to watersheds with characteristics similar to the CCW, and (2) an "adjusted parameter set" with modifications to input parameters related to evapotranspiration, soil water storage, and soil water lateral flow. Comparisons of daily, average monthly, and annual average simulated and observed flows for the 1997-2005 simulation period using the base parameter set resulted in Nash-Sutcliffe efficiency (E_{NS}), root mean square deviation (RMSD), and relative error (PBIAS) coefficients of 0.34 to 0.48 for E_{NS}, 1.50 to 8.79 m^3 s^{-1} for RMSD, and -18.43% for PBIAS. All statistical evaluation coefficients improved for the adjusted parameter set (e.g., 0.44 to 0.59 for E_{NS}, 0.87 to 7.73 m^3 s^{-1} for RMSD, and -8.59% for PBIAS). The ranges of E_{NS} and PBIAS values for uncalibrated or manually adjusted streamflow predictions in this study (using both parameter sets) were similar to others reported in the literature for various watershed models. This study represents the first attempt to develop and apply a complex natural resource system model under the OMS. The results indicate that the OMS-J2K watershed model was able to reproduce the hydrological dynamics of the CCW and should serve as a foundation on which to build a more comprehensive model to better quantify water quantity and quality at the watershed scale. In particular, the topological routing scheme employed by OMS-J2K (thus allowing the simulation of lateral processes vital for the modeling of runoff concentration dynamics) is much more robust than the quasi-distributed routing schemes used by other watershed-scale natural resource models and represents a noteworthy advancement in hydrological modeling toward deriving suitable conservation management scenarios.*

Keywords. *Fully distributed modeling, Hydrologic modeling, Model evaluation, Object Modeling System, Streamflow, Watershed.*

The problems facing both users and developers of environmental models are becoming increasingly complex. Environmental management issues related to ecology (e.g., habitat restoration), hydrology (e.g., water management), and agricultural management practices (e.g., fertilizer and pesticide application) become compounded when viewed within the physical, biological, chemical, and geological responses of the natural world. It can be argued that achieving the goal of sustainable environmental management should involve consideration of whole-system effects. Unfortunately, as Ahuja et al. (2005) point out, ecological systems typically involve highly complex interactions of soil, plant, weather, and management components that are extremely difficult to quantitatively describe. Thus, challenges in optimal resource management have created demand for state-of-the-art, integrated, flexible, and easy-to-use modeling tools that are able to simulate the quantitative and qualitative aspects of environmental processes (e.g., the hydrologic cycle) with a sufficient degree of reli-

Submitted for review in February 2011 as manuscript number SW 9072; approved for publication by the Soil & Water Division of ASABE in January 2012.

USDA is an equal opportunity provider and employer.

The authors are **James C. Ascough II, ASABE Member,** Research Hydrologic Engineer, USDA-ARS Agricultural Systems Research Unit, Fort Collins, Colorado; **Olaf David,** Research Associate, Departments of Civil and Environmental Engineering and Computer Science, Colorado State University, Fort Collins, Colorado; **Peter Krause,** Program Director, Thuringian State Institute for Environment and Geology, Jena, Germany; **Gary C. Heathman,** Research Soil Scientist, USDA-ARS National Soil Erosion Research Laboratory, West Lafayette, Indiana; **Sven Kralisch,** Research Assistant, Department of Geography, Friedrich Schiller Universität, Jena, Germany; **Myriam Larose, ASABE Member,** Research Fellow, School of Natural Resources and Environment, University of Michigan, Ann Arbor, Michigan; **Lajpat R. Ahuja, ASABE Member,** Research Soil Scientist, USDA-ARS Agricultural Systems Research Unit, Fort Collins, Colorado; and **Holm Kipka,** Research Associate, Department of Civil and Environmental Engineering, Colorado State University, Fort Collins, Colorado. **Corresponding author:** James C. Ascough II, USDA-ARS Agricultural Systems Research Unit, Fort Collins, CO 80526; phone: 970-492-7371; fax: 970-492-7310; e-mail: jim.ascough@ars. usda.gov.

ability. Although a large number of environmental simulation models are available, they are typically constrained to the specific scales and purposes they have been developed for and therefore are more robust in some areas than others (depending on the primary goal guiding their development). Furthermore, most of the existing models are monolithic and not modular; they are very difficult to update, extend, or connect with other models; and they lack the flexibility to meet current needs for more integrated analysis of dynamic environmental issues (David et al., 2002).

All of the above reasons indicate a need for a comprehensive model development framework that can integrate existing and future environmental models into a common, collaborative, interoperable, and flexible system. Such a system should embrace a modular design for simulation models that reduces code complexity and supports reusability and compatibility of embedded science modules, ultimately resulting in more efficient collaborative (and interdisciplinary) modeling efforts. The system should be able to integrate different categories of applications potentially requiring different levels of scientific detail and comprehensiveness, as driven by problem objectives, scale of application, and data constraints. The Object Modeling System (OMS) currently being developed by the USDA-ARS Agricultural Systems Research Unit and Colorado State University (Fort Collins, Colo.) has been designed to meet the above criteria. OMS (David et al., 2002) provides a component-based modeling framework that allows the implementation of single- or multi-process modules that can be developed and applied as custom-tailored model configurations. It has some advantages over other existing environmental modeling frameworks, e.g., Open Modeling Interface (OpenMI, Gregersen et al., 2007), Earth System Modeling Framework (ESMF, Hill et al., 2004), and the Framework for Risk Analysis in Multimedia Environmental Systems (FRAMES, Castleton and Gelston, 2003), in that it has integrated capabilities for module and model building, database access, model calibration, and geospatial output visualization. Furthermore, OMS is entirely Java-based and therefore can operate on major computing platforms.

In addition to the growing interest in environmental modeling frameworks (Rizzoli et al., 2008), recent advances in computing capability and geographical information systems (GIS) have led to increasingly sophisticated watershed-scale models that incorporate climatic, soil, topographic, and land use characteristics and are capable of addressing multiple issues related to water quantity and quality concerns and environmental assessments (Heathman et al., 2009). Notable examples of continuous watershed simulation models include the Soil and Water Assessment Tool (SWAT) (Arnold et al., 1993) and the Annualized Agricultural Nonpoint-Source Pollution (AnnAGNPS) model (Yuan et al., 2001). The value of these types of computer models in solving problems related to water quantity and quality in the last decade is reflected by directives and programs like the Conservation Effects Assessment Project (CEAP) in the U.S. and the EU-Water Framework Directive (WFD) in Europe. CEAP is comprised of two main components (Duriancik et al., 2008): (1) a national assessment conducted by the USDA-NRCS that provides model estimates of conservation benefits for annual reporting, and (2) a watershed assessment study conducted by the USDA-ARS aimed at quantifying the environmental benefits from specific conservation practices at the watershed scale (Mausbach and Dedrick, 2004). The five-year ARS CEAP Watershed Assessment Study (WAS) Project Plan (USDA-ARS, 2004) provides detailed descriptions of research studies at 14 benchmark watersheds in the U.S., each of which has a particular area of special emphasis due in part to watershed location and regional water quality issues. There are five major objectives of the WAS portion of CEAP; the primary goal of Objective 5 is to "develop and verify regional watershed models that quantify environmental outcomes of conservation practices in major agricultural regions," with a sub-objective to "extract relevant scientific components from legacy software such as SWAT, AnnAGNPS, or other models as appropriate, and integrate them into OMS" (USDA-ARS, 2004). Thus, in order to satisfy the requirements of CEAP WAS Objective 5, a new watershed model development approach is needed that can take full advantage of OMS modeling framework capabilities for assembling appropriate modules into a model customized to a specific problem and scale of application for a region. In order to address the overall goal of CEAP (e.g., quantify the impacts of implementing conservation practices at field to large watershed scales), the model should be applicable to large watersheds or river basins of more than 500 km^2 and also provide the ability to model the hydrological cycle in a spatially distributed and process-oriented manner. The European J2000 model (Krause et al., 2006) was selected to provide the initial components for a regionalized watershed model that satisfies the above CEAP requirements. J2000 (referred to hereafter as J2K) is an object-oriented, hydrological system for fully distributed simulation of the water balance in large watersheds and catchments. It was initially developed in the C++ programming language, converted to Java, and has been previously evaluated in a number of catchments in Germany (Krause, 2002; Krause et al., 2006) and South Africa (Scheffler et al., 2005). J2K was selected to provide initial regionalized watershed model components because of its object-oriented programming structure (essential when considering the future goal of integrating additional science components from SWAT, AnnAGNPS, and other models) and because the fully distributed topological flow routing scheme utilized by J2K is applicable at drainage areas ranging from tens to thousands km^2 and much more robust than flow routing schemes used by other watershed-scale natural resource models.

The specific objectives of this study were to: (1) implement J2K hydrological modeling components under the OMS, (2) assemble a new modular watershed-scale model for fully distributed transfer of water between land units and stream channels, and (3) evaluate the accuracy and applicability of the modular watershed model for estimating streamflow. The Cedar Creek watershed (CCW) in northeastern Indiana was selected for application of the OMS-based watershed model. The CCW is within the larger St. Joseph River watershed, and is the largest tributary of the St. Joseph River, which supplies drinking water for approximately 250,000 people (SJRWI, 2004) in the city of Fort Wayne, Indiana. The St. Joseph River watershed (SJRW) was designated in 2004 as one of the CEAP benchmark watersheds. Approximately 76% of the SJRW is under extensive agricultural production. In order to achieve initial development phase goals for the OMS-based watershed model, it was deemed important to initially assess model performance in estimating streamflow only (i.e., the focus was on accurate representation of the hydrological system rather than on water quality). In addition, a decision was made to first apply the model without formal (e.g., autocalibration) calibration methods, thus eliminating uncertainties related to the use of different optimized model parameter values. This research is unique in that it represents the first attempt to develop and apply a complex natural resource system model under the OMS. In addition, this study represents first time that J2K hydrological process components have been evaluated on a watershed in the U.S.

The Object Modeling System (OMS)

OMS version 2.2 represents a comprehensive ARS-led effort in partnership with the NRCS, the U.S. Geological Survey (USGS), and university collaborators (e.g., Colorado State University). Modular environmental frameworks for model development like OMS are well-suited for comprehensive projects like the CEAP WAS that require complex simulation component technology integrated into a common, collaborative, and flexible system (Ascough II et al., 2005). The basic (component-based) concept is the representation of all system and model components as independent entities coupled by software interfaces (David et al., 2002). In order to achieve maximum platform independence, OMS 2.2 was implemented in the Java programming language and on top of the NetBeans application platform. Extension of OMS 2.2 using new system components was facilitated through NetBeans integration because of the flexible and generic design of this platform.

The principal architecture of OMS 2.2 is presented in figure 1. OMS 2.2 core system components include reusable features such as simulation control across time and space, auxiliary tools for model calibration, and control of data input/output. OMS 2.2 modeling tools, such as the Component Builder and Model Builder, support model development whereby multiple scientific components can be assembled into a complex model (fig. 1). Science model components usually implement specific approaches for representing environmental processes, e.g., water balance, plant growth, chemical transport, flow routing, etc. The Component Builder supports development of scientific Java components and also allows the adaptation of legacy source code written in the Fortran and C/C++ programming languages. The Model Builder supports visual integration and configuration of complex models from standalone model components with an easy-to-use graphical user interface that offers capabilities for mapping component output to the input of subsequent components. With the Model Builder, different model configurations can be stored and managed. Once a model has been assembled and configured inside the Model Builder, it can be easily passed to other users or executed in other computing environments. OMS 2.2 also provides various tools for model data analysis, such as statistical evaluation and plotting/geospatial visualization capabilities (fig. 1). Various 2-D plots are available that can be used to display input data and model output responses for various simulation runs, such as a component that allows visualization and manipulation of spatial GIS data using NASA WorldWind geospatial technology. The above tools and components are fully integrated within the OMS 2.2 framework to enable a project-oriented modeling process, i.e., within OMS 2.2, a modeling project can be defined to accommodate all modeling resources such as components, models, input parameter files, observed data (for statistical evaluation), and simulation scenarios. The OMS 2.2 platform is currently evolving into OMS3 (David et al., 2010), which offers a more lightweight approach (i.e., less framework-specific code is required) for component and model integration. The general component code and model structure that was used for this study still exists; however, execution management and framework interoperability are improved under OMS3.

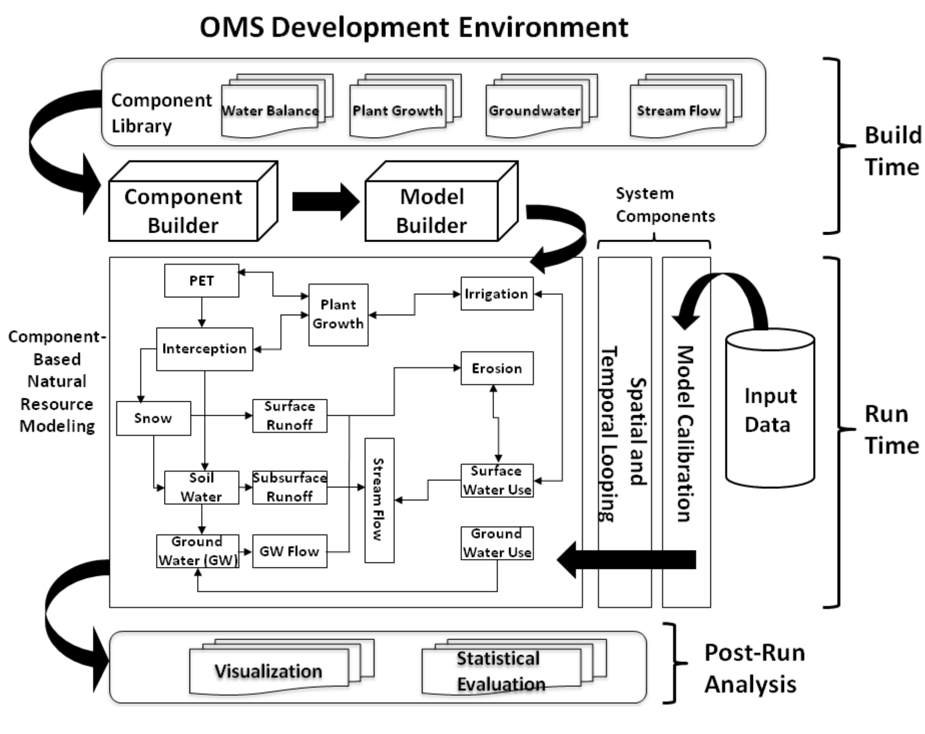

Figure 1. Detailed schematic of major OMS 2.2 framework components including OMS model, system, and science module components.

The J2K Watershed Model

The J2K modeling system (Krause, 2002; Krause et al., 2006) was used for the simulation of the hydrological dynamics of the Cedar Creek watershed in Indiana. J2K is a modular, spatially distributed hydrological system that implements hydrological processes as encapsulated process components. J2K operates at various temporal (either hourly or daily time steps) and spatial aggregation levels throughout the watershed. For example, the generation of four separate runoff components, i.e., surface runoff (RD1), interflow from the unsaturated soil zone (RD2), interflow from the saturated weathering layer of the underlying hydro-geological unit (RG1), and saturated baseflow (RG2) is simulated inside the modeling core of J2K for each hydrologic response unit (HRU) (fig. 2) with subsequent calculation of runoff concentration processes (through a lateral routing scheme) and flood routing in the stream channel network. An overview of J2K functionalities for the preprocessing of input data (e.g., regionalization of climate data such as precipitation and temperature from point sources) and a description of the major hydrological processes simulated are given in the following sections.

J2K Climate Data Preprocessing

Regionalization methods are implemented for transformation of climate data collected at a point (e.g., precipitation, minimum and maximum air temperature, wind speed, relative humidity, and solar radiation) into spatially distributed data sets. These methods analyze the vertical (e.g., decrease of temperature with increasing elevation) and horizontal (e.g., horizontal variation of rainfall) variability of each data set for each time step (Krause, 2002). Vertical variability is quantified by a linear regression between station elevation and parameter value, providing a daily gradient and coefficient of determination (R^2). If the R^2 value is greater than a user-defined threshold, the parameter values are adapted to the elevations of the discrete subareas by the gradient of the regression line. Using this approach, vertical variability is only considered for data values showing a significant correlation with the elevation at the specific time step. Horizontal variability is quantified by an inverse distance weighting method. The combination of the two regionalization functions results in new climate input values for each day and discrete HRU. The use of a more sophisticated regionalization method, such as the one described here, is indispensable for macro-scale hydrological modeling because it reproduces the larger heterogeneity of the spatial distribution of climate input data much better than the monthly lapse rates or Thiessen-polygon approaches often found in hydrological models, which are typically only suitable for small catchments with less spatial heterogeneity of input data (Krause et al., 2006).

The regionalized climate input data sets are then used as J2K driving parameters, together with the physiogeographic parameters of each HRU derived from the GIS data layers. J2K first determines whether the precipitation is falling as snow or rain (or a mixture of rain and snow) by a probability function determined from the air temperature on which 50% of the precipitation falls as rain and 50% as snow. Around this probability distribution, a temperature interval is calculated with an upper temperature threshold above which only rain occurs and a lower threshold below which the entire precipitation occurs as snowfall. Between these thresholds, rain-snow mixtures with variable percentages for each component are calculated. The resulting precipitation is then passed to modules for interception, snow processes, and soil water balance.

Plant Interception and Evapotranspiration

The interception module (fig. 2) uses a simple storage approach according to Dickinson (1984), which calculates a maximum interception storage capacity based on the leaf area index of the respective land use. As long as this maximum capacity is not exceeded, precipitation is stored in the actual interception storage, which is depleted by evaporation. When the maximum storage capacity is exceeded, any surplus of rainfall is treated as throughfall and passed to the other modules. Potential evapotranspiration (PET) is calculated

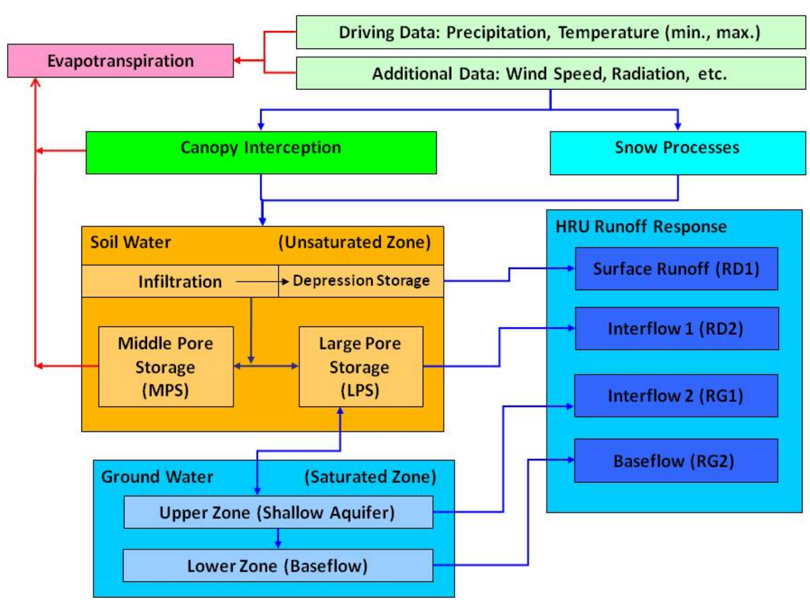

Figure 2. Conceptual diagram of the OMS-J2K model showing critical storages and processes.

according to the Penman-Monteith method (Monteith, 1975a, 1975b) which uses the regionalized climate data information and the parameters of the specific vegetation class for each HRU. The implemented Penman-Monteith approach takes climatic constraints, (e.g., temperature, radiation, and wind speed) as well as specific parameters (e.g., aerodynamic resistance, bulk resistance, and effective height) of different vegetation types into account. The seasonal dynamics of the vegetation parameters are derived throughout the year by continuous functions extrapolated from discrete values taken from various literature sources. Actual evapotranspiration (AET) is calculated based on the PET and the actual soil moisture using either a linear or a nonlinear reduction function.

Snow Processes

The snow module (fig. 2) combines both empirical and physically based routines, and simulates accumulation and compaction of the snowpack caused by snowmelt or rain-on-snow precipitation events. For this purpose, the water-equivalent of the dry snow (and the related density) and the water-equivalent of the dry snow plus the stored liquid water and density of the whole snowpack are calculated for each time step. This approach allows J2K to better simulate the ability of the snowpack to store large amounts of liquid water without necessarily producing snowmelt runoff. J2K differentiates both the snow accumulation phase and the compaction and melt phase during the lifetime of the snowpack. The model switches between these phases depending on the air temperature. If the temperature is lower than the specific temperature threshold and the entire precipitation falls as snow, then only the accumulation phase is active. If the temperature is above the second threshold (where the entire precipitation falls as rain), then only the settling and melt phase is active. Both phases are active between the two phases, allowing the modeling of both snow accumulation and melt within one time step.

Soil Water Processes

The most complex part of J2K is the soil water balance module, which reflects the primary role of the soil zone as a regulation and distribution system and interacts with nearly all other J2K process modules. A schematic of the soil water balance module is shown in figure 2. An empirical approach has been implemented in J2K to reproduce surface runoff flow (RD1) resulting from snowmelt on frozen soils (or inside the snowpack) and from infiltration excess during rainfall with high intensity. Central to the empirical approach is a unique storage water concept based on two different compartments for the soil profile unsaturated zone (fig. 2). The first storage compartment is the middle pore storage (MPS), describing the water storage capacity of the middle-sized pores (diameter = 0.2 to 50 μm) in which stored water is held against gravity and can only be drained by an active tension. The MPS storage capacity corresponds to the usable field capacity of the soil. The second compartment is the large pore storage (LPS), describing the water storage capacity of the large pores and macropores (diameter >50 μm), which are not able to hold water against gravity and are the primary source for any vertical and horizontal outflows. The LPS storage capacity corresponds to the air capacity of the soil. The storage capacity of the MPS and LPS compartments is determined by the description of the soil profiles together with the effective rooting depth of the land use class for each HRU.

A threshold value for the maximum infiltration capacity can be set by the user and is weighted during the simulation with the relative saturation of the MPS soil water storage compartment, resulting in an actual infiltration rate:

$$inf_{act} = \left(1 - \theta_{\mathrm{MPS}}\right) \cdot inf_{max} \tag{1}$$

where inf_{act} is the actual infiltration rate reduced according to the relative storage content of the MPS (mm d^{-1}), θ_{MPS} is the MPS soil water storage content, and inf_{max} is a user-defined maximum infiltration rate (mm d^{-1}). Any water exceeding the actual infiltration rate is passed to surface depression storage from where it can either produce surface runoff or remain available for infiltration until the next time step (depending on the slope of the specific HRU). Rainfall or snowmelt on impervious areas also results in surface runoff. J2K distinguishes land use classes of impervious areas with a grade of sealing of 80% or greater (i.e., urban areas) or less than 80% (i.e., agricultural/rural areas). The percentage of water directly contributing to surface runoff for the above two categories can be modified by the user.

The distribution of infiltrated water between the MPS (MPS_{in}, mm d^{-1}) and LPS (LPS_{in}, mm d^{-1}) storage compartments is calculated using the relative saturation of the MPS as an indicator (i.e., the more saturated this storage component is, the less water it receives, and vice versa):

$$\mathrm{MPS}_{in} = inf_{act} \cdot \left(1 - \mathrm{e}^{-dist/\theta_{\mathrm{MPS}}}\right) \tag{2}$$

$$\mathrm{LPS}_{in} = inf_{act} - \mathrm{MPS}_{in} \tag{3}$$

where *dist* is a user-defined calibration parameter. This approach ensures that the LPS always receives some part of the infiltrated water, except if the MPS is completely depleted during the preceding time step. Using this method, vertical or horizontal runoff can occur before field capacity is reached. Therefore, fast runoff resulting from preferential flow paths or macropores is often reproduced much better than by more common methods in which runoff can only occur after FC is saturated. The MPS is depleted by transpiration of the vegetation cover only. The amount of water removed by the vegetation depends on the actual evapotranspiration deficit and the relative saturation of the MPS, whereby the maximum AET is calculated using either a linear or a nonlinear, logistic relationship between the above two variables.

As previously stated, the LPS storage compartment is the source of vertical and horizontal flows occurring inside the unsaturated soil profile. The total amount of outflow from LPS ($\mathrm{LPS}_{outflow}$, mm d^{-1}) is calculated by a nonlinear relationship taking the relative saturation of the storage into account:

$$\mathrm{LPS}_{outflow} = \mathrm{LPS}_{act} \cdot \left(\theta_{\mathrm{LPS}}\right)^{\mathrm{LPS}_{out}} \tag{4}$$

where LPS_{act} is the actual LPS storage content, θ_{LPS} is the LPS soil water storage content, and LPS_{out} is a user-defined calibration parameter. The total amount of outflow is then distributed to horizontal (interflow, RD2) and vertical (percolation) components, with the contribution to each of the components calculated by taking geomorphological (e.g., slope) as well as pedological (e.g., hydraulic conductivities, thickness of soil horizons) parameters into account:

$$\text{Interflow} = \text{LPS}_{outflow} \cdot \tan\alpha \cdot latVertDist \quad (5)$$

$$\text{Percolation} = \text{LPS}_{outflow} \cdot (1 - \tan\alpha) \cdot latVertDist \quad (6)$$

where α is the HRU slope (m m^{-1}), and *latVertDist* is a user-defined calibration parameter. If the HRU is linked to a highly saturated groundwater storage zone, the percolation rate is reduced and the excess is passed back to the LPS. If there is still water left in the LPS after the subtraction of the percolation and interflow components, this amount is partly used for replenishing the MPS (depending on its actual relative saturation).

Groundwater Processes

The groundwater domain is conceptualized by two storages, RG1 and RG2, for each HRU (fig. 2). RG1 represents the water movement in the shallower withering zone of the bedrock, and RG2 represents the water movement in the deeper aquifer and/or in fractures and is synonymous with baseflow. The water input (i.e., percolation) into the groundwater module from the LPS is distributed among the two storages based on slope and a calibration parameter. Outflow from the two RG storages is calculated from the actual storage content, a recession coefficient, and another calibration parameter.

Lateral and Stream Channel Routing

After calculation of the RD1, RD2, RG1, and RG2 runoff generation processes, runoff concentration is computed based on topological interconnections of the single HRU polygons, i.e., water fluxes are modeled as flow cascades from the headwaters down to a connected stream segment. The lateral routing can be derived very easily because the hydrograph recession of the flow components during lateral routing has already been taken into account in the soil water and groundwater process modules. Each of the four runoff components generated on single HRU polygons are passed to a receiving HRU defined by its topological position (derived by GIS analysis) or to a receiving stream reach (if the HRU is connected to one). The flood routing inside the stream network is simulated by connecting the reach storages receiving the water from the topologically connected HRUs by a hierarchical storage cascade and calculating the flow velocity inside the streambed with the Manning-Strickler equation. For each stream reach, the user has to define the flow length (*len*, m), bed width, bed slope (s_o, m m^{-1}), and Manning's roughness (n) in the reach parameter input file. The module assumes a simple rectangular streambed shape and calculates the actual flow velocity by an iterative approach. From the current flow in the stream reach (q_{act}, m^3 s^{-1}) and the bed width, a hydraulic radius (r_h, m) is calculated. With this hydraulic radius, a velocity (v, m s^{-1}) is determined according to Manning-Strickler:

$$v = \frac{1}{n} \cdot s_o^{1/3} \cdot r_h^{2/3} \quad (7)$$

The values of r_h and v are iteratively calculated until the change in flow velocity between iterations is smaller than 0.001 m s^{-1}. With this flow velocity, a flood routing recession coefficient (r_k, unitless), dependent on the flow length of the stream reach (*len*, m) and a user-defined routing coefficient (t_a, h), is calculated:

$$r_k = \frac{v}{len} \cdot t_a \cdot 3600 \quad (8)$$

Finally, the stream reach outflow (m^3 s^{-1}) is calculated:

$$\text{Stream}_{out} = q_{act} \cdot e^{(-1/r_k)} \quad (9)$$

The outflow of the specific stream reach is then transferred as inflow to the downstream reach.

JAMS-J2K to OMS-J2K Migration

The J2K model has previously been implemented only in the JAMS (Jena Adaptable Modelling System) modeling framework (Kralisch and Krause, 2006). Therefore, as shown in figure 3, the following J2K modeling resources needed to be transferred to the OMS framework:

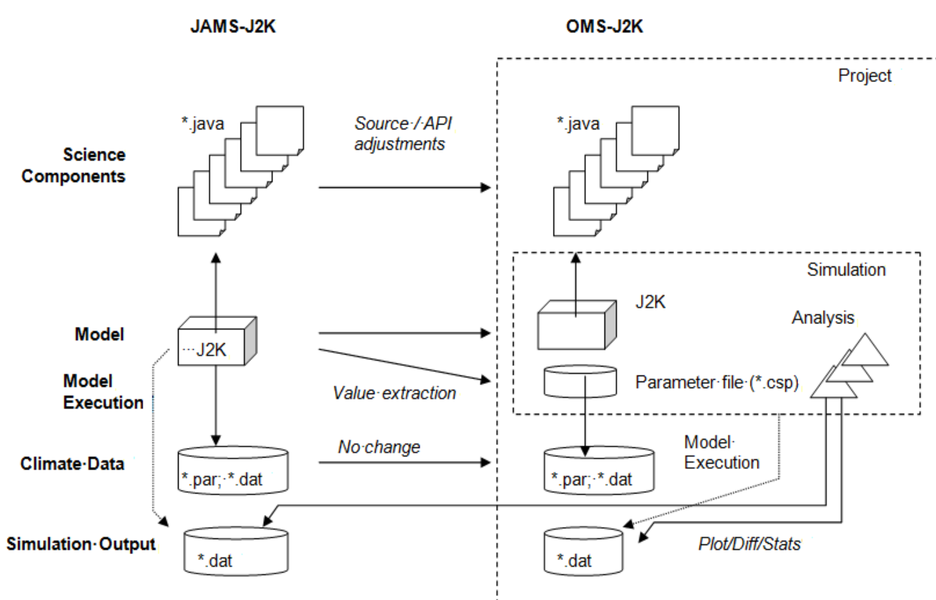

Figure 3. JAMS-J2K to OMS-J2K migration path.

- 40+ J2K Java scientific source components for hydrological process representation on a watershed scale, including climate regionalization, overland flow, infiltration, evapotranspiration, soil water movement, groundwater storage, and flood routing as described in the previous section.
- XML (Extensible Markup Language) model file descriptions for J2K component use, connectivity, and execution order. Default values for watershed-specific parameters are defined here.
- ASCII data input files for hydrogeology, soils, land use, HRU routing, and channel reach routing that are referenced from the J2K model XML file.

Although the J2K model is object-oriented, implementation under the OMS framework provides additional benefits in terms of component reusability and substitutability, as well as access to OMS auxiliary tools (e.g., output visualization). J2K migration was facilitated by the fact that the JAMS modeling framework originated from an earlier version of the OMS. Changes in scientific code were kept as minimal as possible, i.e., only required changes for framework adjustments were performed. Several processing scripts were used to semi-automate this migration, and all J2K resources (e.g., components, model, data, etc.) were migrated from the J2K reference base using the following steps:

1. All JAMS framework dependencies were removed, and JAMS data types and annotations were replaced with OMS attributes and annotations. Component interfaces and methods were transformed (all other component information stayed). This process was 95% automated through the use of pattern matching scripts.
2. The JAMS J2K model XML file was duplicated using the OMS Model Builder, i.e., attributes and spatial data structures representing the fully distributed approach in J2K were created using the Model Builder. Components were integrated as defined in the original J2K model with respect to their execution order and attribute connectivity. Additional descriptive information about the components was added to the model.
3. All climate input data files were kept in their original form and structure since all science components for data input were also transformed from JAMS. Data output was implemented using the OMS Application Programming Interface (API). OMS property parameter sets (*.csp) containing default parameter settings for the Cedar Creek watershed were created.

In addition to the migration of J2K science components, the XML model file, and I/O parameter files, the following OMS-specific resources were created to support the migration process: (1) a simulation control file was created for the Cedar Creek watershed to link the OMS-J2K model to the proper parameter file and related analysis descriptors, and (2) several analysis files for major state variables were created to compare the original JAMS-J2K output against OMS-J2K output based on identical input parameter settings and climate input. The analysis files were executed during model runtime and produced various time series plots, scatter plots, and difference plots of JAMS-J2K vs. OMS-J2K output data.

Materials and Methods

Study Area

The Cedar Creek watershed (CCW) is located within the St. Joseph River basin in northeastern Indiana (41° 10′ 10″ to 41° 32′ 38″ N, 84° 53′ 49″ to 85° 19′ 44″ W) and covers Noble, DeKalb, and Allen counties. The CCW drains two 11-digit hydrologic unit code (HUC) subwatersheds, Upper Cedar Creek (04100003080) and Lower Cedar Creek (04100003090), covering an area of approximately 700 km^2 (fig. 4). The average land surface slope of the watershed is 2.6%, and topography varies from rolling hills in Noble county to nearly level plains in DeKalb and Allen counties, with minimum and maximum altitudes above sea level of 232 m and 326 m, respectively. Soil types on the watershed were formed from compacted glacial till, and the predominant soil textures are silt loam, silty clay loam, and clay loam (SJRWI, 2004). The annual mean precipitation in the watershed area from 1989 to 2005 was 962 mm. The average temperature during crop growth seasons ranges from 10°C to 23°C. The watershed is mainly used for farmland and livestock production and is characterized by a high percentage of rotationally tilled agricultural row crops (48.9%, which mainly consist of corn, soybean, and winter wheat including 5.3% fallow), grassland (e.g., ryegrass) (27.4%), woodland (12.4%), and pasture/CRP (Conservation Reserve Program) (7.9%). The major land cover types are evenly distributed throughout the watershed except the ryegrass and pasture/CRP. The pasture/CRP concentrates mainly in the northern and western parts, while ryegrass is concentrated in the central eastern part.

CCW Soil Types and Land Use

The interaction and aggregation of soil and land use GIS data layers in OMS-J2K at the HRU level play an important role in describing the hydrologic response of the system in a realistic manner (Heathman et al., 2009). In the CCW, eight STATSGO soil associations are represented (fig. 5a). STATSGO polygon IN004 (52.9% of the watershed area) is dominated by the Crosby and Treaty soil series, Blount-Glynwood-Morley; STATSGO polygon IN005 (26.7%) is

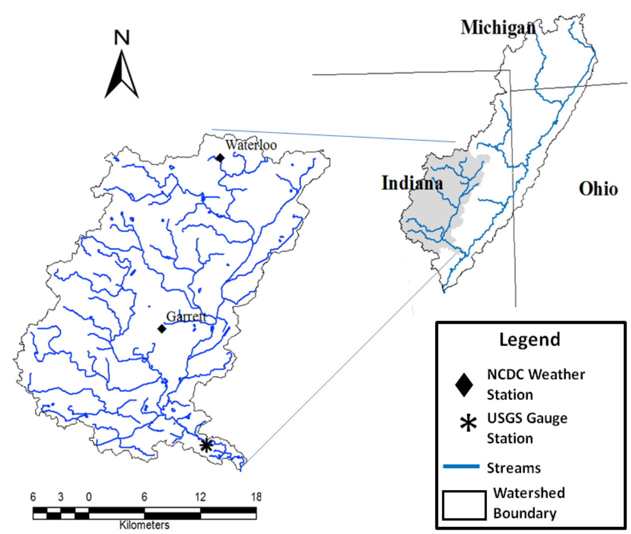

Figure 4. Cedar Creek watershed stream network, weather stations, and USGS gauging station for OMS-J2K modeling.

Table 1. STATSGO soil associations in the Cedar Creek watershed.

Soil	Texture	Hydrologic Soil Group	Area (km^2)	Area (%)
Blount-Glynwood-Morley (IN004)	Silt loam	C	374.0	52.9
Blount-Pewamo-Glynwood (IN005)	Silt loam	C	189.0	26.7
Miami-Wawasee-Crosier (IN016)	Silt loam-Loam	B	48.5	6.9
Houghton-Adrian-Carlisle (IN019)	Silt loam	B	25.2	3.6
Sebewa-Gilford-Homer (IN025)	Silt loam	B	56.5	7.9
Martinsville-Whitaker-Rensselaer (IN028)	Loam	B	14.4	2.0
Total			707.6	100.0

comprised primarily of the Crosby and Cyclone soil series, Blount-Pewamo-Glynwood; STATSGO polygon IN025 (7.9%) is dominated by Sebewa-Gilford-Homer; IN016 (6.9%) is dominated by Miami-Wawasee-Crosier; IN019 (3.6%) is comprised of Houghton-Adrian-Carlisle; and IN028 (2.0%) is comprised of Martinsville-Whitaker-Rensselaer (table 1). STATSGO polygons IN007 and IN029 comprise almost negligible area and were not considered.

For this study, a land use map from the USDA National Agricultural Statistics Service (NASS) was used. The NASS land use map (USDA-NASS, 2001) is a raster, geo-referenced, and categorized land use data layer produced using satellite imagery from the Thematic Mapper (TM) instrument on Landsat 5 and the Enhanced Thematic Mapper (ETM+) on Landsat 7. The land use data were collected between the dates of 29 April and 5 September 2001 with an approximate scale of 1:100,000 and a ground resolution of 30 × 30 m. The remotely sensed land use data are used to produce a GIS data layer that is interfaced with OMS-J2K as model input. The NASS 2001 land use categories were reclassified into eleven OMS-J2K land use categories. As listed

Table 2. NASS 2001 land use for the Cedar Creek watershed.

Land Use	NASS 2001 Area (km^2)	NASS 2001 Area (%)
Agricultural row crops[a]		
Corn	121.2	17.1
Soybeans	175.9	24.9
Winter wheat	4.3	0.6
Other small grains and hay	6.1	0.9
Double-cropped winter wheat/soybeans	0.8	0.1
Popcorn	0.2	0.03
Fallow/idle cropland	37.4	5.3
Pasture/grassland/non-agriculture	249.5	35.3
Deciduous forest	88.8	12.4
Evergreen forest	--	--
Mixed forest	--	--
Woods[b]	--	--
Urban	16.8	2.4
Transportation/commercial	--	--
High-density residential	--	--
Low-density residential	--	--
Water	5.6	0.9
Wetlands	1.0	0.1
Total	707.6	100.0

[a] Values in **bold** represent OMS-J2K land use categories.
[b] OMS-J2K considers two categories of woods.

in table 2 and shown in figure 5b, the major percentages of land use as input into J2K are agricultural row crops (49%, including reclassification of fallow), pasture (35%), and forests (12%). Pastureland is comprised of grassland used for grazing and hay (27.4%) and land enrolled in conservation programs such as the Conservation Reserve Program (CRP) (7.9%). A small fraction of open water and urban areas make up the remaining land use.

HRU Delineation and Flow Routing

For hydrological modeling of the runoff dynamics of the Cedar Creek watershed, the watershed boundary, stream channel network, physiographic hydrological response units (HRUs), and topological (flow) connections between HRUs

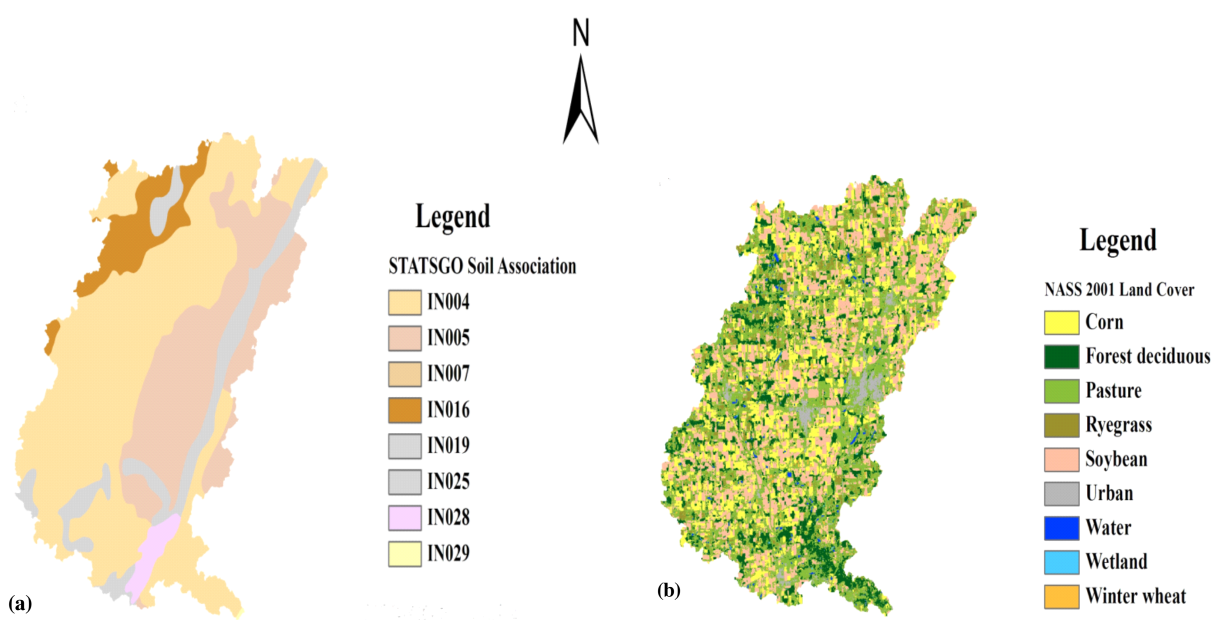

Figure 5. (a) STATSGO database GIS soil map layer, and (b) NASS 2001 GIS land use map layer.

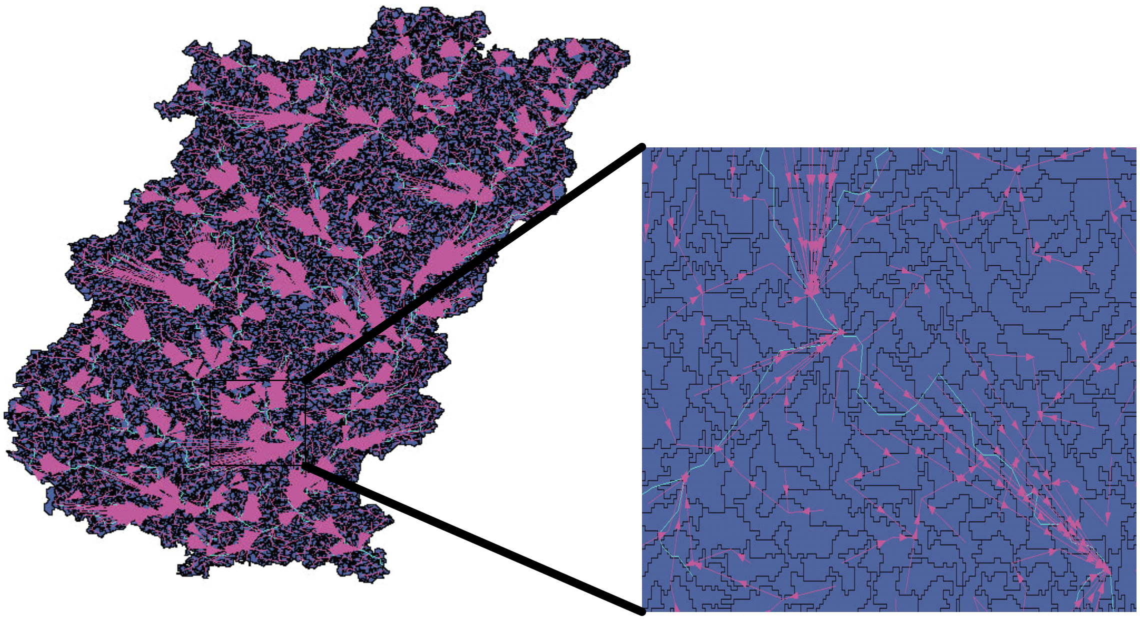

Figure 6. Routing topology with overland flow routing vectors for the Cedar Creek watershed including an expanded view of flow routing vectors with HRU and stream channel flow linkages.

were delineated using ArcGIS 9.2 (Environmental Systems Research Institute, Redland, Cal.). Both standard ArcGIS geoprocessing tools (e.g., overlay) and customized scripts for deriving HRU flow connectivity were used. The delineation was based on GIS layers derived from digital elevation model (DEM) data and the STATSGO soil type and reclassified NASS land use maps as described above; there is no limit to the number of HRUs that can be delineated. The DEM data used in this study were obtained from the USGS at 10 m elevation resolution, 1/3 arc second, and a map scale of 1:24,000 quadrangle sheet. The DEM was projected to Universal Transverse Mercator (UTM) NAD83, Zone 16 north for the state of Indiana.

For final HRU delineation, the DEM topographical parameters (e.g., elevation, slope, aspect) were partly reclassified and combined (by overlay analysis in ArcGIS 9.2) with the STATSGO soil and NASS land use GIS layers. The resulting unique polygons were then aggregated (based on their attribute set and neighborhood proximity) to reduce the overall number of spatial HRU entities. The delineation of HRUs for the entire Cedar Creek watershed resulted in 4,174 HRU polygons featuring areas between 0.02 to 2.5 km^2. A script for the topological routing scheme was derived in ArcGIS 9.2 for the simulation of lateral runoff generation processes, which determines the watershed spatial connections (e.g., HRU to HRU and HRU to stream reach). Figure 6 shows the stream channels and HRU polygons of the Cedar Creek watershed, together with topological connections as red arrows draped over the HRU polygons. From figure 6, the dynamic spatially distributed character of the OMS-J2K HRU flow routing approach that separates this model from other watershed models (e.g., SWAT) becomes apparent.

OMS-J2K Model Parameterization

The OMS-J2K simulation period was 11 years (1995-2005); however, the first two years were not used for model evaluation in order to allow model parameters to reach equilibrium with actual physical conditions (Santhi et al., 2001; Fontaine et al., 2002). Daily precipitation and maximum/minimum air temperatures were obtained from the National Oceanic and Atmospheric Administration National Climate Data Center (NOAA-NCDC, 2004) for the Garret and Waterloo weather stations for the years 1995-2005 (see fig. 4 for CCW station locations). Data for solar radiation, wind speed, and relative humidity were generated using the WGEN (Richardson and Wright, 1984) stochastic weather generator. As described previously, the regionalization preprocessors in OMS-J2K automatically distributed the climate data from the two gauges over the watershed. Historical measured data for Cedar Creek streamflow gauge 04180000 (41° 13′ 8″ N, 85° 4′ 35″ W) (fig. 4) were supplied by the USGS for the nine-year evaluation period from January 1997 to December 2005.

The OMS-J2K parameters describing a watershed and its hydrological response can be considered as spatially distributed but temporally static descriptors (or spatial attributes) that describe spatial heterogeneity and variability in the watershed. The spatial attributes of the CCW (e.g., elevation, slope, aspect, soil type ID, land use type ID) for each HRU polygon were derived as previously discussed and stored along with the flow routing information in an HRU topology parameter file. In a second parameter file, physical soil parameters (e.g., air capacity, field capacity) are defined according to the horizon description of the STATSGO soil map for each soil type. In a third parameter file, physical vegetation parameters (e.g., LAI, albedo, stomatal resistance, effective height, and effective rooting depth) are stored for each land use class. Effective parameters describing the groundwater domain (storage capacity and recession coefficients for the aquifer system) are contained in a fourth parameter file. The interaction between the parameter files is described by the spatial relationship between the soil and land use IDs in the HRU topology parameter file and the respective (i.e., matching) IDs in the other parameter files. During the model initialization sequence, this information is read from the files and transferred as spatial attributes to the HRU and stream reach objects of the model.

Table 3. OMS-J2K input parameters used for base parameter set simulations.

	Parameter	Description	Recommended Range	Parameter Value
General initialization	*FCAdaptation*	Multiplier for field capacity	0.0 to 5.0	1.0
	ACAdaptation	Multiplier for air capacity	0.0 to 5.0	1.0
	initRG1	Initial storage of RG1 relative to maximum storage	0.0 to 1.0	0.50
	initRG2	Initial storage of RG2 relative to maximum storage	0.0 to 1.0	0.50
Interception	*a_rain*	Maximum storage capacity per LAI for rain (mm)	0.0 to 10.0	2.5
	a_snow	Maximum storage capacity per LAI for snow (mm)	0.0 to 10.0	3.0
Snow	*snow_trs*	Upper temperature threshold above which only rain occurs (°C)	0.0 to 0.5	0.0
	snow_trans	Lower temperature threshold below which only snow occurs (°C)	-2.0 to 2.0	1.0
	baseTemp	Melting temperature of snow (°C)	-1.0 to 1.0	0.3
	t_factor	Temperature factor for snowmelt calculation	0.0 to 5.0	0.85
	r_factor	Rain factor for snowmelt calculation	0.0 to 5.0	0.25
	g_factor	Soil heat factor for snowmelt calculation	0.0 to 10.0	2.0
	snowCritDens	Snowpack density beyond free water is released (g cm^{-1})	0.1 to 1.0	0.40
	ccf_factor	Cold content factor	0.0 to 1.0	0.10
Soil water	*soilMaxDPS*	Maximum depression storage capacity (mm)	0.0 to 10.0	2.0
	soilPolRed	Potential reduction coefficient for AET computation	0.0 to 10.0	5.0
	soilLinRed	Linear reduction coefficient for AET computation	0.0 to 10.0	0.0
	soilMaxInfSummer	Maximum infiltration rate in summer (mm d^{-1})	0.0 to 200.0	100.0
	soilMaxInfWinter	Maximum infiltration rate in winter (mm d^{-1})	0.0 to 200.0	75.0
	soilMaxInfSnow	Maximum infiltration rate for snow covered areas (mm d^{-1})	0.0 to 200.0	40.0
	soilImpGT80	Relative infiltration for impervious areas greater 80% sealing	0.0 to 1.0	0.25
	soilImpLT80	Relative infiltration for impervious areas less 80% sealing	0.0 to 1.0	0.60
	soilDistMPSLPS	MPS/LPS distribution coefficient	0.0 to 10.0	1.5
	soilDiffMPSLPS	MPS/LPS diffusion coefficient	0.0 to 10.0	2.0
	soilOutLPS	Outflow coefficient for LPS	0.0 to 10.0	3.0
	soilLatVertLPS	Lateral/vertical distribution coefficient for LPS	0.0 to 10.0	1.0
	soilMaxPerc	Maximum percolation rate (mm d^{-1})	0.0 to 20.0	5.0
	soilConcRD1	Recession coefficient for overland flow	0.0 to 10.0	1.7
	soilConcRD2	Recession coefficient for interflow	0.0 to 10.0	2.0
Groundwater	*gwRG1RG2dist*	RG1/RG2 distribution coefficient	0.0 to 1.0	0.80
	gwRG1Fact	Adaptation of RG1 outflow	0.0 to 10.0	1.0
	gwRG2Fact	Adaptation of RG2 outflow	0.0 to 10.0	1.0
	gwCapRise	Capillary rise coefficient	0.0 to 1.0	0.0
Flood routing	*flowRouteTA*	Flood routing coefficient controlling flood wave velocity	0.0 to 100.0	1.0

In addition to the files containing spatial attributes as described above, the *.csp file (as described in the JAMS-J2K to OMS-J2K Migration section and shown in fig. 3) contains non-spatial parameters describing coefficients used in OMS-J2K initialization, interception, snow processes, soil water, groundwater, and flood routing science module components. Initial OMS-J2K parameter values and recommended ranges are listed in table 3 and were taken from simulation studies successfully applying JAMS-J2K to watersheds in Germany and elsewhere exhibiting physical characteristics (e.g., topography, size, and agricultural land use) very similar to the CCW. The "base parameter set" presented in table 3 represents an initial attempt to establish realistic input parameter values without resorting to a detailed calibration procedure. In addition to the base parameter set, an "adjusted parameter set" was also developed to better account for evapotranspiration dynamics and tile drainage areas in the CCW. This was accomplished by adjusting three OMS-J2K input parameters controlling the amount of PET partitioned to AET, the amount of water available in the LPS soil water storage compartment, and the rate of outflow from the LPS soil water storage compartment. All OMS-J2K CCW simulations were run using both the base and adjusted parameter sets.

OMS-J2K Model Statistical Evaluation

Four evaluation criteria were used to assess daily, monthly, and average annual streamflow simulated by OMS-J2K. The criteria are quantitative statistics that evaluate the overall correspondence of simulated output to observed values and include the Nash-Sutcliffe efficiency coefficient (E_{NS}), coefficient of determination (R^2), root mean square deviation (RMSD), relative absolute error (RAE), and percent bias (PBIAS). The E_{NS}, RMSD, RAE, and PBIAS statistics are defined as:

$$E_{NS} = 1 - \frac{\sum_{i=1}^{n} (O_i - P_i)^2}{\sum_{i=1}^{n} (O_i - \bar{O})^2} \tag{10}$$

$$\text{RMSD} = \sqrt{\frac{\sum_{i=1}^{n} (O_i - P_i)^2}{n}} \tag{11}$$

$$\text{RAE} = \frac{\sum_{i=1}^{n} \left| O_i - P_i \right|}{\sum_{i=1}^{n} \left| O_i - \overline{O} \right|} \tag{12}$$

$$\text{PBIAS} = \frac{\sum_{i=1}^{n} \left(P_i - O_i \right) \cdot 100.0}{\sum_{i=1}^{n} O_i} \tag{13}$$

where P_i is the ith value of streamflow (m^3 s^{-1}) predicted by the OMS-J2K model, O_i is the ith observed value of streamflow (m^3 s^{-1}), $\overline{O}$ is the average observed streamflow during the simulation period (m^3 s^{-1}), and n is the number of observations. E_{NS} indicates how well the plot of observed versus simulated values fits a 1:1 line. The value of E_{NS} in equation 9 may range from $-\infty$ to 1.0, with 1.0 representing a perfect fit of the data. E_{NS} values were computed for both monthly and daily streamflow. The coefficient of determination (R^2) represents a measure of the strength of the linear relationship between predicted streamflow and observed measurements, whereas the RMSD is indicative of the error associated with estimated streamflow. RAE is the total absolute error relative to what the total absolute error would have been if the prediction had been the mean of the observed values. PBIAS is a measure of the average tendency of simulated streamflows to be larger or smaller than corresponding observed values. The optimal PBIAS value is 0.0; a positive value indicates a bias toward overestimation, whereas a negative value indicates a model bias toward underestimation. The PBIAS evaluation statistic has been presented by Gupta et al. (1999) and others in the literature with a positive value indicating model bias towards underestimation and a negative value indicating bias towards overestimation. However, we find this to be counterintuitive, which explains the slightly different form of equation 13 presented herein. Donigan et al. (1984) considered the Hydrological Simulation Program - Fortran (HSPF) model performance for a monthly time step very good if the absolute percent error is less than 10%, good if the error is between 10% and <15%, and fair if the error is between 15% and <25% for calibration and validation. In a review of model evaluation criteria by Moriasi et al. (2007), model performance for a monthly time step was judged to be satisfactory if PBIAS is less than ±25% and E_{NS} is greater than 0.50. Van Liew et al. (2005) suggest that for both daily and monthly time steps, PBIAS values less than ±20% are considered good, values between ±20% and ±40% are considered satisfactory, and values greater than ±40% are considered unsatisfactory. In addition, Van Liew et al. (2005) consider E_{NS} values greater than 0.75 good, values between 0.75 and 0.36 satisfactory (Motovilov et al., 1999), and values less than 0.36 unsatisfactory. Given the fact that formal calibration techniques were not used, the Van Liew et al. (2005) standard, which is somewhat more relaxed than the Moriasi et al. (2007) standard, was adopted for the E_{NS} and PBIAS evaluation criteria used in this study. In addition to assessing model performance based on the criteria mentioned above, Tukey's least significant difference (LSD) statistical test was also used at the $\alpha = 0.05$ level to analyze statistical differences between observed and simulated average streamflow values.

RESULTS

Historical measured data for Cedar Creek streamflow from the USGS for a nine-year period (January 1997 to December 2005) at gauge 04180000 (41° 13′ 8″ N, 85° 4′ 35″ W) near Cedarville, Indiana, were compared with daily, monthly, and annual OMS-J2K noncalibrated streamflow. The streamflow data obtained from the USGS are composed of baseflow and surface runoff; therefore, no baseflow filter program was applied to the OMS-J2K streamflow predictions.

BASE PARAMETER SET SIMULATIONS

Although the OMS-J2K model was run uncalibrated using the base parameter set, modeled water balance predictions for the simulation period (e.g., evapotranspiration, surface runoff) were compared with historical averages that are representative of hydrologic conditions on the watershed. The Indiana Department of Natural Resources (IDNR, 1980, 1987) reported that the long-term average annual net supply to surface water in the northeastern part of the state is 305 mm, distributed as 213 to 229 mm in diffused surface water and 76 to 91 mm in recharge to groundwater. The average annual precipitation in this part of Indiana is approximately 965 mm, with ET accounting for approximately 660 mm (IDNR, 1980, 1987). For the base parameter set, average annual measured precipitation on the CCW was 922 mm, OMS-J2K average annual simulated ET was 688 mm, and OMS-J2K average annual simulated surface runoff was 201 mm.

Daily observed and OMS-J2K simulated streamflow from January 1997 to December 1997 and from January 2000 to December 2000 are presented in figures 7 and 8, respectively. These graphs serve as one-year subsets of the results from the nine-year simulation period and represent the highest (1997) and lowest (2000) annual average streamflow years for the CCW during the simulation period. For uncalibrated conditions, overall model performance on a daily time step was quite variable (unsatisfactory to good based on the evaluation statistics in table 4); however, the trend in streamflow appeared to be captured correctly. There were significant and frequent underestimations (and some overestimations) by the OMS-J2K model on some days compared to the measured data, which may be due in part to having rainfall input data for only two weather stations in the CCW. Heathman et al. (2009) reported that daily rainfall records for the Garret and Waterloo weather stations show many periods of time when significant rainfall events were recorded (with a subsequent response or spike in simulated streamflow data using the SWAT model), yet little or no response was observed in the USGS discharge data at the watershed outlet. They hypothesized that these were extremely localized rainfall events that did not significantly contribute to the total measured watershed streamflow.

As with the Heathman et al. (2009) study, the OMS-J2K modeled distribution of rainfall over the entire watershed area was based on input data from the Garret and Waterloo weather stations. In general, the OMS-J2K model underestimated streamflow on a daily time step, as shown in the 1:1 scatter plot in figure 9, where all data points are included for the nine-year simulation period. The negative value for PBIAS (-18.43%) indicates that the model underestimated streamflow, and the E_{NS} (0.34) and R^2 (0.48) values are con-

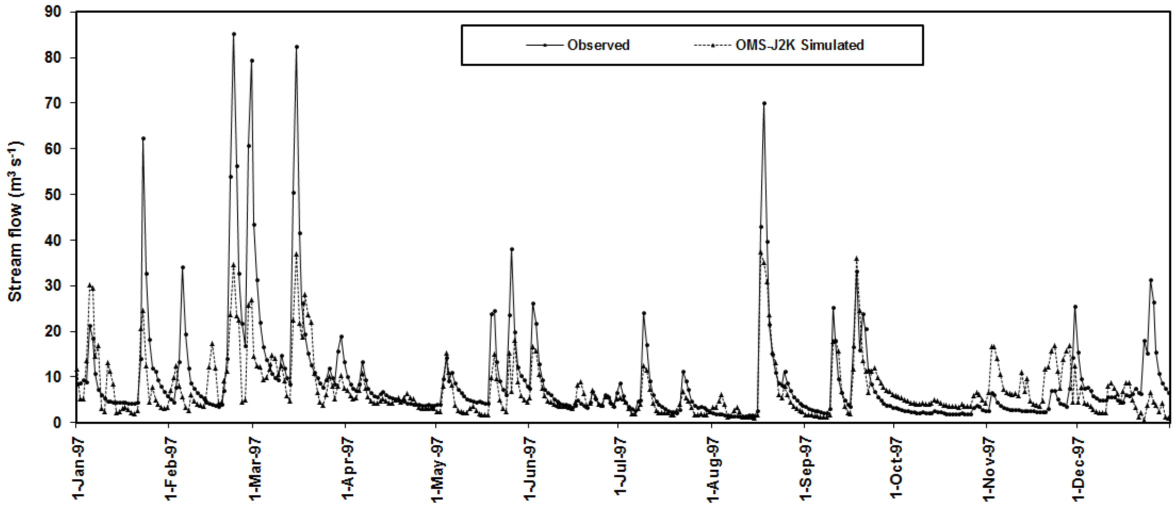

Figure 7. Daily Cedar Creek watershed streamflow for observed and OMS-J2K base parameter set simulated values (January 1997 to December 1997).

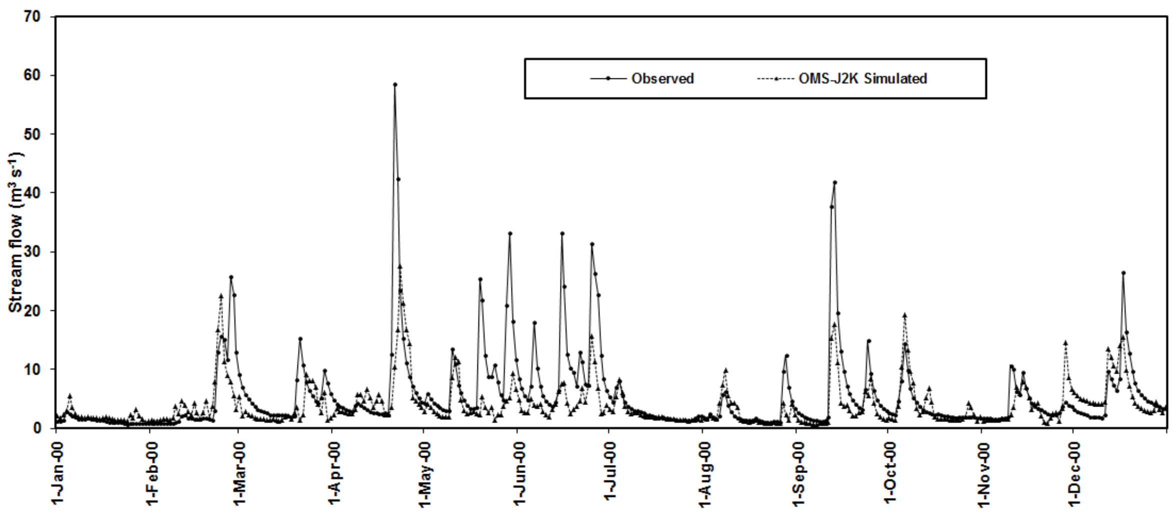

Figure 8. Daily Cedar Creek watershed streamflow for observed and OMS-J2K base parameter set simulated values (January 2000 to December 2000).

Table 4. Statistical evaluation for OMS-J2K simulated daily, average monthly, and average annual Cedar Creek watershed streamflow (January 1997 to December 2005).[a]

Statistical Evaluation Coefficient	Base Parameter Set			Adjusted Parameter Set		
	Daily Streamflow	Average Monthly Streamflow	Average Annual Streamflow	Daily Streamflow	Average Monthly Streamflow	Average Annual Streamflow
E_{NS}	0.34	0.48	0.44	0.44	0.59	0.52
R^2	0.48	0.69	0.82	0.54	0.77	0.87
RMSD	8.79	4.10	1.50	7.73	3.21	0.87
RAE	0.64	0.54	1.38	0.60	0.43	0.75
PBIAS	-18.43			-8.59		

[a] E_{NS} = Nash-Sutcliffe efficiency, R^2 = coefficient of determination, RMSD = root mean square deviation (m^3 s^{-1}), RAE = relative absolute error, and PBIAS = bias or relative error (%).

sidered unsatisfactory according to Van Liew et al. (2005), although the PBIAS value is good since it is less than ±20%. The RMSD and RAE values for daily streamflow were 8.79 m^3 s^{-1} and 0.64, respectively. The results of Tukey's LSD test (α = 0.05) for the difference between observed and simulated streamflow are given in table 5. The base parameter set results for the 1997 and 2000 daily streamflow analysis show that simulated daily streamflow for these two years are significantly different from the observed daily streamflow.

Average monthly observed and J2K simulated streamflow from January 1997 to December 2005 are presented in figure 10. This figure shows that the trend in simulated average monthly streamflow followed the observed values much

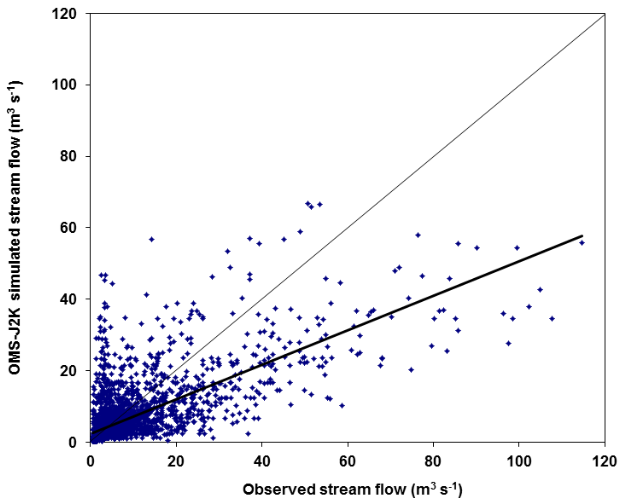

Figure 9. Daily Cedar Creek watershed streamflow 1:1 plot of OMS-J2K base parameter set simulated values versus observed (January 1997 to December 2005).

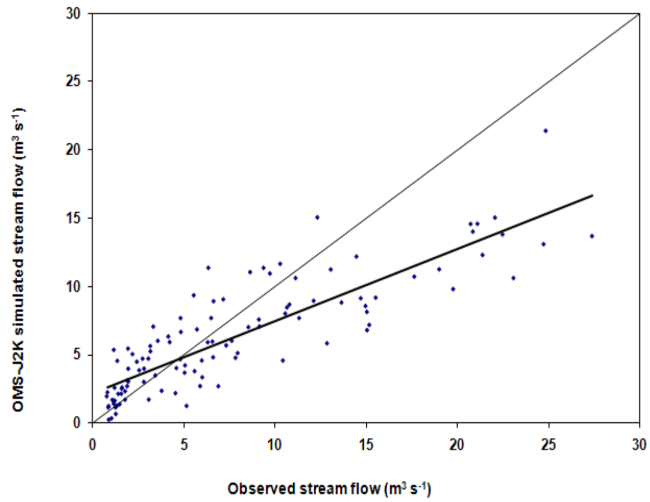

Figure 11. Monthly Cedar Creek watershed streamflow 1:1 plot of OMS-J2K base parameter set simulated values versus observed (January 1997 to December 2005).

Table 5. Tukey's LSD analysis for observed and OMS-J2K simulated daily (1997 and 2000) and average annual Cedar Creek watershed streamflow.[a]

	Daily Streamflow (1997) (m^3 s^{-1})	Daily Streamflow (2000) (m^3 s^{-1})	Average Streamflow (all years) (m^3 s^{-1})
Observed	9.42 a	5.55 a	7.70 a
OMS-J2K (base parameter set)	7.83 b	4.48 b	6.28 b
OMS-J2K (adjusted parameter set)	9.09 a	5.14 a	7.04 b

[a] Average values followed by the same letter are not significantly different using Tukey's LSD test with α = 0.05.

more closely than the simulated daily streamflow results. Furthermore, it is easy to discern that the simulated average monthly streamflow in figure 10 was significantly underestimated for most of the nine-year simulation period. This significant underestimation trend is also readily apparent in the monthly 1:1 streamflow scatter plot shown in figure 11. The statistical results for average monthly streamflow in table 4 show that E_{NS} improved to 0.48, the RMSD (4.10 m^3 s^{-1}) was less than half of the daily streamflow, and the RAE decreased to 0.54. The PBIAS value for average monthly streamflow is not shown as it is essentially the same as for daily streamflow. Similar to the results for daily streamflow, the average monthly streamflow results in table 5 for Tukey's test (α = 0.05) also indicate a significant difference between the observed and OMS-J2K simulated streamflow values.

The data for average annual observed and simulated streamflow are shown in figure 12 for the nine-year simulation period; the simulated data clearly indicate the strong OMS-J2K underprediction for all years. OMS-J2K model performance based on the statistical analysis in table 4 indicates that streamflow simulation results at the annual output time scale were generally better than simulation results for the daily and monthly output time scales, with the exception of E_{NS}, which decreased to 0.44. The results for Tukey's LSD test (α = 0.05) in table 5 again show that the simulated annual average streamflow values were significantly different from the observed annual average values. As expected, the RMSD continued to decrease with increasing time scale, i.e., average annual streamflow RMSD (1.50 m^3 s^{-1}) was again less than half of the average monthly streamflow RMSD. It should be noted that on a year-by-year basis, the data in figure

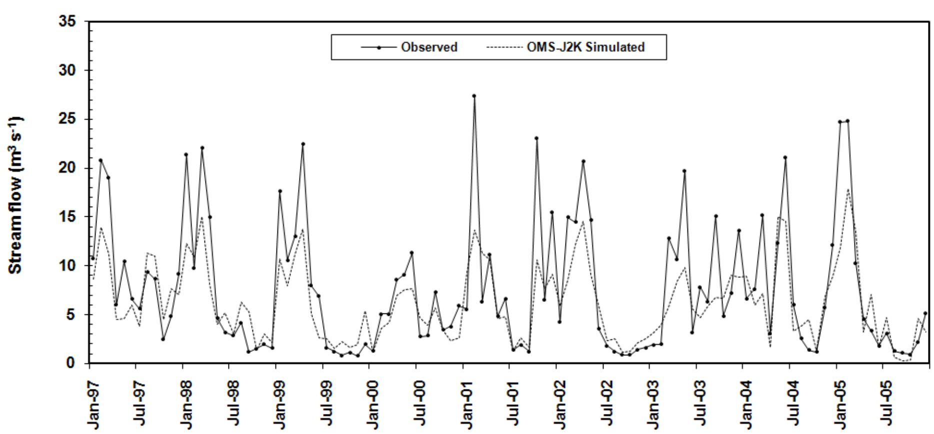

Figure 10. Monthly Cedar Creek watershed streamflow for observed and OMS-J2K base parameter set simulated values (January 1997 to December 2005).

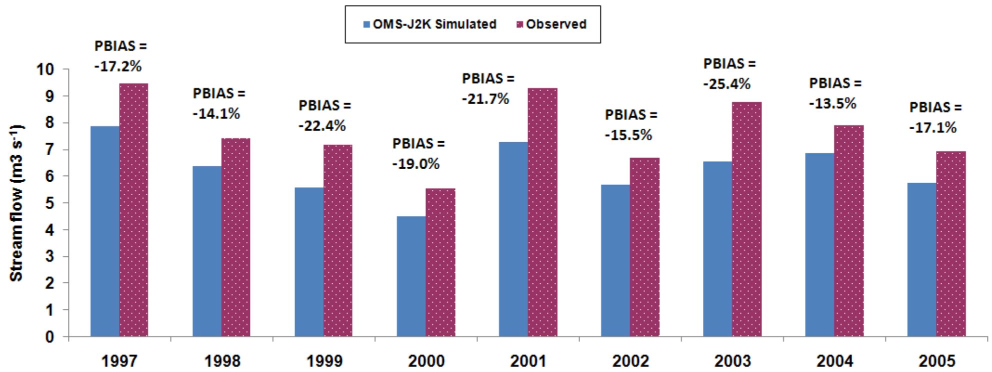

Figure 12. Annual average Cedar Creek watershed streamflow for observed and OMS-J2K base parameter set simulated values (January 1997 to December 2005).

12 indicate that simulated average annual streamflow was underestimated somewhat randomly across the simulation period and was generally unaffected by the magnitude of observed streamflow. However, closer inspection of the data shows that the three years with the lowest observed streamflows (2000, 2002, and 2005; average streamflow of 6.4 m^3s^{-1}) were underestimated to a lesser degree by OMS-J2K (-17.2% average underestimation) than the three years with the highest observed streamflows (1997, 2001, and 2003; average streamflow of 9.2 $m^3\ s^{-1}$), with the observed streamflow underestimated by an average of -21.4% (data not shown).

Finally, figure 13 shows E_{NS}, R^2, and RAE values computed from the simulated (using the base parameter set) and observed monthly streamflows for individual years (fig. 13a) and cumulatively at a one-year increment (fig. 13b) for the entire 1997-2005 simulation period. With the exception of 2000 (the year with the lowest observed streamflow), the E_{NS} and R^2 evaluation statistics are fairly consistent across the simulation period (fig. 13a). Interestingly, the RAE evaluation statistic is much higher than the E_{NS} and R^2 evaluation statistics, predominantly for the years with the lowest observed (e.g., 2000 and 2005) and highest observed (e.g., 1997 and 2001) streamflows (fig. 13a). For the cumulative E_{NS}, R^2, and RAE evaluation statistics (fig. 13b), large fluctuations occur during the first five years of the simulation period (1997-2001) and stabilize for the remaining four years (2002-2005).

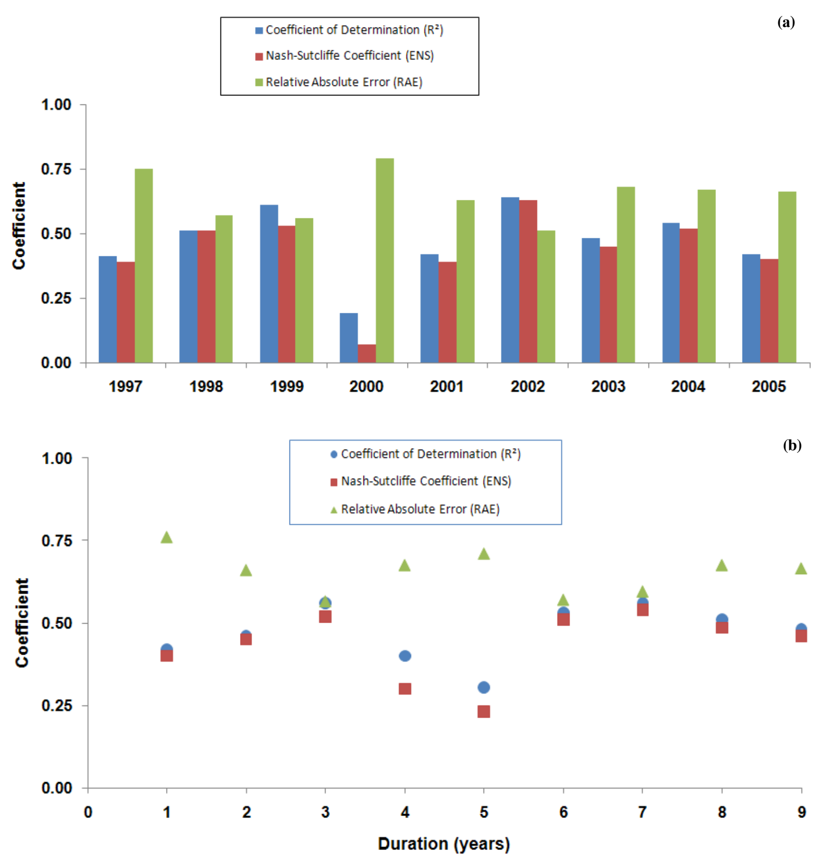

Figure 13. Comparative evaluation statistics for J2K-OMS base parameter set simulated values and observed monthly flows for the Cedar Creek watershed (January 1997 to December 2005): (a) individual years, and (b) cumulative years.

Adjusted Parameter Set Simulations

The simulation results presented for the base parameter potentially indicate overprediction of ET on the watershed in addition to a systematic underprediction of streamflow across all time scales. Table 1 shows that land use on the watershed is quite diverse; furthermore, the simplistic representation of evapotranspiration dynamics in OMS-J2K may not adequately capture complex soil water and plant interactions occurring in the watershed. Therefore, the *soilLinRed* coefficient in table 3 was increased from 5.0 to 8.0. This coefficient controls the partitioning of PET to AET, i.e., increasing *soilLinRed* decreases the amount of PET partitioned to AET. In addition, an attempt was made to account for areas of tile drainage on the Cedar Creek watershed. A logical way to represent the effects of tile drainage in OMS-J2K was to increase both the amount of water available in the LPS and the rate of outflow from LPS. Therefore, the *soilDistMPSLPS* and *soilOutLPS* coefficients (table 3) were decreased from 1.5 to 0.50 and from 3.0 to 1.0, respectively. Decreasing *soilDistMPSLPS* increases the amount of infiltrated water available for LPS; decreasing *soilOutLPS* increases the outflow rate from LPS. These adjustments approximate the more rapid removal of water from tile drains than what would normally be expected with the absence of tile drainage. All OMS-J2K CCW simulations were re-run using the new "adjusted parameter set" with the modified values for *soilLinRed*, *soilDistMPSLPS*, and *soilOutLPS*. This is similar to the procedure employed by Bosch et al. (2004), who applied the SWAT model from 1997-2002 to a Little River, Georgia, sub-watershed and compared scenarios for default parameter conditions and modified initial conditions. The adjusted parameter set simulation results are presented in tables 4 and 5 and figures 14 and 15.

Table 4 shows that all statistical evaluation coefficients for daily streamflow improved substantially for the adjusted parameter set compared to the base parameter set. In particular, the E_{NS} coefficient increased from 0.34 to 0.44, and PBIAS decreased from -18.43% to -8.59%. The OMS-J2K model still underestimated streamflow on a daily time step (as shown in the 1:1 plots in fig. 14); however, the improvement in scatter around the 1:1 line compared to the base parameter set simulation results in figure 9 is noticeable. Furthermore, the adjusted parameter set results in table 5 for Tukey's LSD test ($\alpha = 0.05$) show that simulated daily streamflow for 1997 and 2000 was not significantly different from observed daily streamflow. Table 4 also shows that all statistical evaluation coefficients for average monthly and average annual streamflow improved for the adjusted parameter set as compared to the base parameter set. Average monthly and average annual improvements were of similar magnitude as the improvements in daily streamflow. However, the adjusted parameter set results in table 5 for Tukey's LSD test ($\alpha = 0.05$) show that simulated streamflow averaged for all years was significantly different from average observed annual streamflow. Average monthly observed and J2K simulated streamflow from January 1997 to December 2005 for the adjusted parameter set are shown in figure 15. This figure shows that the trend in simulated average monthly streamflow for the adjusted parameter set followed the observed values much more closely (both in trend and in better estimation of peak streamflow events) than the simulated monthly streamflow results for the base parameter set shown in figure 10.

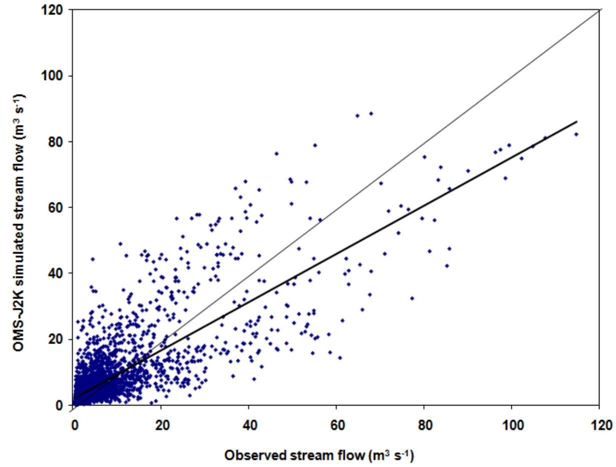

Figure 14. Daily Cedar Creek watershed streamflow 1:1 plot of OMS-J2K adjusted parameter set simulated values versus observed (January 1997 to December 2005).

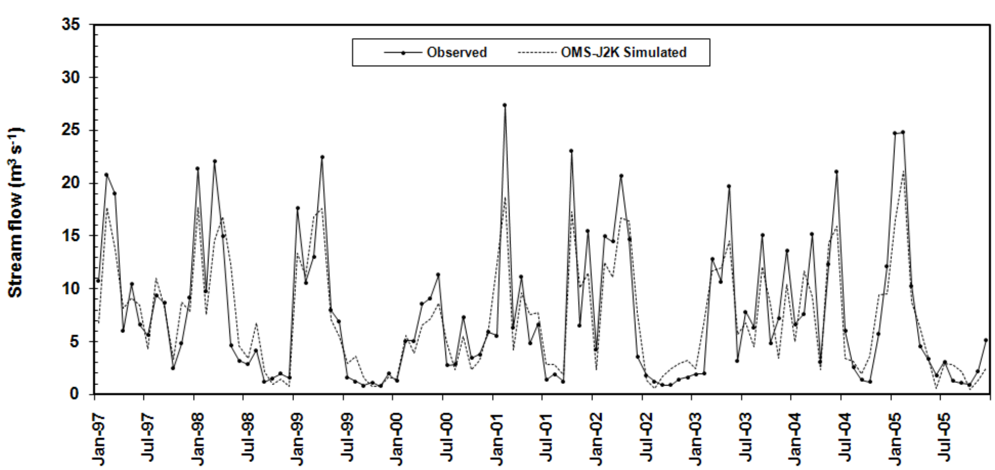

Figure 15. Monthly Cedar Creek watershed streamflow 1:1 plot of OMS-J2K adjusted parameter set simulated values versus observed (January 1997 to December 2005).

Discussion

The range of relative error (e.g., PBIAS) and E_{NS} values for uncalibrated or manually adjusted daily streamflow predictions in this study (for both parameter sets) are similar to others reported in the literature for various watershed models. There is a considerable collection of literature that demonstrates the use of the SWAT model in effectively modeling streamflow (e.g., Van Liew and Garbrecht 2003; Di Luzio et al., 2005; White and Chaubey 2005; Larose et al., 2007). The statistical analysis results reported in this study for uncalibrated daily (PBIAS = -18.43% and -8.59%, E_{NS} = 0.34 and 0.44, and RAE = 0.64 and 0.60 for the base and adjusted parameter sets, respectively), monthly (E_{NS} = 0.48 and 0.59; RAE = 0.54 and 0.43), and annual (E_{NS} = 0.44 and 0.52; RAE = 1.38 and 0.75) streamflow predictions fall within the range of those found throughout the literature. For SWAT daily streamflow predictions, Van Liew and Garbrecht (2003) reported uncalibrated E_{NS} values as low as -7.05 that were improved with calibration to values as high as 0.60 for three subwatersheds in the Little Washita River, Oklahoma, watershed. For a small watershed in Kentucky, Spruill et al. (2000) found that differences between observed and calibrated daily SWAT streamflow rates ranged between ±25% over a two-year period and that the size of the drainage area influenced SWAT discharge prediction accuracy. A five-year study by Wang and Melesse (2006) showed that for the Elm River watershed in North Dakota, calibrated daily SWAT streamflow predictions ranged from 5% overprediction to 35% underprediction compared to the observed data. For SWAT monthly streamflow predictions, Tolson and Shoemaker (2007) reported E_{NS} values ranging from 0.43 to 0.86 for different gauge stations in the Cannonsville Reservoir in upstate New York. Van Liew and Garbrecht (2003) reported uncalibrated SWAT E_{NS} values as low as -4.49 for streamflow that were improved with calibration to values as high as 0.75 for the Little Washita River, Oklahoma, subwatersheds. Bosch et al. (2004) applied the SWAT model to a Little River, Georgia, subwatershed using different input scenarios (low vs. high spatial resolution data and default initial parameters vs. parameters modified for existing groundwater conditions) and obtained E_{NS} values ranging from 0.55 to 0.80 for monthly total flow volumes. Manguerra and Engel (1998) used a non-rigorously calibrated SWAT on a 113.4 km^2 tile-drained Indiana watershed and obtained an E_{NS} of 0.48 and an R^2 of 0.82 for monthly streamflow from 1991 to 1995. Without available information to account for the tile drainage effects, they adjusted the curve number and return flow parameters to offset the impacts of subsurface drainage on the rainfall-runoff response. Parajuli et al. (2009) reported SWAT monthly E_{NS} values for streamflow in a south-central Kansas watershed of 0.56 for calibration and 0.48 for validation. For average annual streamflow, Van Liew and Garbrecht (2003) stated that the SWAT model underestimated streamflow by 18.4% (almost identical to this study) using default values for model parameters affecting streamflow prediction, and on a year-by-year basis SWAT underestimated one year by as much as 98.4% while overestimating another year by 156.9%. Larose et al. (2007) and Heathman et al. (2009) both used the SWAT model to estimate daily, average monthly, and average annual streamflow for the Cedar Creek watershed. Larose et al. (2007) reported E_{NS} coefficients for monthly and daily streamflow calibration and validation ranging from 0.51 to 0.66, respectively. Heathman et al. (2009) reported best model performance values of E_{NS} = 0.58, R^2 = 0.66, and PBIAS = 21.93% for uncalibrated monthly streamflow predictions. OMS-J2K evaluation statistics for streamflow also fall in the same range as those produced using the AnnAGNPS model. Sarangi et al. (2007) used AnnAGNPS to predict runoff and sediment losses from forested and agricultural watersheds on the island of St. Lucia in the Caribbean. Based on calibration and validation of the model for different rainfall events, Sarangi et al. (2007) reported errors of 7% to 36% for annual streamflow prediction from the agricultural watershed, which are higher than the OMS-J2K noncalibrated streamflow PBIAS value in this study (-18.4%). In a two-year study on a small watershed in southern Ontario, Das et al. (2006) reported that AnnAGNPS underestimated mean annual runoff by approximately 55% for noncalibrated conditions, which is again considerably higher than the range of underprediction obtained with OMS-J2K in this study.

Even with streamflow prediction improvements using the adjusted parameter set, OMS-J2K still consistently underestimated streamflow. Because the model time step is daily, it is difficult to accurately capture sub-daily (i.e., individual storms) and even daily results because of potential time shifts in the precipitation and flow data. The addition of a more physically based infiltration component, such as the Green-Ampt infiltration model (Green and Ampt, 1911) used by SWAT and other agroecosystem models, might help in this regard. Streamflow was evaluated on an average monthly and average annual basis (in addition to a daily basis) to better evaluate trends in model output or error; however, OMS-J2K underestimated streamflow at all time scales. Additional possible explanations for the underprediction may be attributed to using default values for the recession coefficient parameters that govern simulated flow through the shallow and deep groundwater storage (RG1 and RG2). Other studies (e.g., Krause, 2002) have shown the J2K model to be particularly sensitive to the recession coefficients (used for final calculation of RG1 and RG2). The CCW streamflow data were simulated without the inclusion of the tile drainage system. Therefore, adjustments to the *soilDistMPSLPS* and *soilOutLPS* coefficients were meant to approximate the effect of tile drainage, i.e., the adjustments approximate the more rapid removal of water from tile drains than what would normally be expected with the absence of tile drainage. Unquestionably, the presence of tile drains significantly impacts the water yield and streamflow in the CCW and addition of a tile drainage component to OMS-J2K should increase streamflow prediction accuracy. Finally, potholes, reservoirs, ponds, and impoundment structures are not currently simulated by OMS-J2K. Some of these structures, particularly ponds and impoundments, are present on the CCW and most likely affect the overall runoff concentration dynamics on the watershed.

The availability of accurate climate data also plays an important role in model performance and accuracy. The effects of spatial and temporal variability in rainfall on model output uncertainty has been previously documented (Haan, 1989; Chaubey et al., 1999), and spatial variability of precipitation data represents one of the major limitations in large-scale hydrologic modeling (Arnold et al., 1998). Hoblit et al. (1999) presented National Weather Service guidelines that recommend seven point-based climate stations to simulate a 1,200 km^2 basin (i.e., one station for every 171 km^2). The

HRUs in OMS-J2K accessed data from only two weather stations in the CCW (fig. 5), one of which (the Waterloo weather station) was on the northernmost boundary of the watershed. As a result, it is possible that the distribution of rainfall over the entire watershed may be inaccurately represented, i.e., an important limitation of the modeling exercise was the spatial resolution of the climate data (which would thus impact streamflow estimation). The streamflow simulation results for OMS-J2K almost certainly would improve if additional stream gauge and weather data (e.g., NEXRAD data) were available.

A large number of studies investigating SWAT model performance for average monthly streamflow have noted that the model tended to underestimate flows during the winter and spring wet months and overestimate flows during the summer and fall dry months (e.g., Feyereisen et al., 2007; Van Liew et al., 2007). Arnold et al. (2000) discussed the occurrence of a seasonal trend (underestimation in spring, overestimation in fall) in SWAT runoff prediction, which they attributed to snowmelt simulation, seasonal variation in ET, and soil moisture variations. As previously discussed, in this study OMS-J2K underestimated the three years with lowest observed streamflows (2000, 2002, and 2005) by an average of 17.2% and underestimated the three years with highest observed streamflows (1997, 2001, and 2003) by an average of 21.4%. Underprediction of streamflow (especially during the spring to summer months, fig. 11) is probably due to an overestimation of ET. The Penman-Monteith equation, which is used in OMS-J2K to estimate ET, requires significant data, including, but not limited to, solar radiation, wind speed, soil characteristics, and canopy cover characteristics. Because only precipitation and temperature were available as historical input data, the other meteorological data needed for this calculation were obtained by using the WGEN weather generator. Considerable uncertainty exists in weather generation, and this uncertainly is propagated in the final ET values determined by OMS-J2K. Furthermore, a lack of available measured ET data for the study period makes it difficult to validate simulated ET results. Under- or overestimations of ET could thereby affect the overall water balance, particularly during the summer months when ET demand is higher (Heathman et al., 2009).

In summary, we chose to evaluate uncalibrated streamflow results considering that OMS-J2K was developed for applications on ungauged watersheds. Tolson and Shoemaker (2007) and Heathman et al. (2009) both caution the potential for formal model calibration to introduce a level of bias that could ultimately mask or eliminate the impact of the simulated runoff generation processes on the simulated streamflow results. In particular, Tolson and Shoemaker (2007) state "The calibration step ... will often be able to mask or eliminate some of the prediction inaccuracies due to incorrect or inaccurate model inputs such as slope and soil inputs." Furthermore, Heathman et al. (2009) point out that "based on previous watershed modeling studies using the SWAT model, it is very likely that nearly all of the simulation years could be calibrated to within satisfactory levels of performance." A shuffled complex evolution (SCE) calibration component (Duan et al., 1992, 1993) has been integrated within OMS-J2K, and future modeling efforts will investigate model predictive performance for streamflow using parameters derived through autocalibration.

Summary and Conclusions

The long-term continuous hydrologic simulations of OMS-J2K performed reasonably well in predicting daily, monthly, and annual average flows on the Cedar Creek (gauge 04180000) near Cedarville, Indiana. Comparisons of daily, monthly, and annual average simulated and observed flows for the 1997-2005 simulation period using a default base parameter set resulted in a relative error of -18.43% for PBIAS and statistical evaluation coefficients ranging from (worst to best) 0.34 to 0.48 for Nash-Sutcliffe efficiency (E_{NS}), 0.48 to 0.82 for coefficient of determination (R^2), and 0.64 to 1.38 for relative absolute error (RAE). Base parameter set values related to PET partitioning, MPS/LPS partitioning, and LPS outflow were subsequently modified to form an adjusted parameter set. All statistical evaluation coefficients for daily, average monthly, and average annual streamflow improved substantially for the adjusted parameter set (e.g., relative error of -8.59% for PBIAS and statistical evaluation coefficients ranging from (worst to best) 0.44 to 0.59 for E_{NS}, 0.54 to 0.87 for R^2, and 0.60 to 0.75 for relative absolute RAE. For both parameter sets, OMS-J2K underpredicted the majority of the peak flows during the nine-year simulation of the Cedar Creek watershed, with some individual storm events underpredicted by many orders of magnitude. Despite the underprediction, all of the evaluation statistics for E_{NS} and PBIAS for both parameter sets were within the good to satisfactory ranges as suggested by Van Liew et al. (2005), with the exception of the daily streamflow E_{NS} value. Furthermore, the range of E_{NS} and PBIAS values for streamflow predictions in this study using both parameter sets were similar to other uncalibrated or manually adjusted streamflow evaluation results reported in the literature for different watershed models. It was unclear whether OMS-J2K needs enhancements in storm event simulations for improving high and peak flow predictions (e.g., addition of a tile drainage component or improved ET component) or whether the distribution of rainfall over the entire watershed was inaccurately represented due to the use of only two climate stations.

The results indicate that the OMS-J2K watershed model was able to reproduce the hydrological dynamics of the Cedar Creek watershed and should serve as a foundation on which to build a regionalized model that is able to quantify the impact of conservation practice implementation on water quantity and quality at the watershed scale. In particular, the topological routing scheme employed by OMS-J2K (thus allowing the simulation of lateral processes important for the modeling of runoff concentration dynamics) is much more robust than the quasi-distributed routing schemes used by other watershed-scale natural resource models (e.g., SWAT). The largest advantage of the OMS-J2K routing approach is a process-oriented view of spatial watershed characteristics that drive hydrological behavior. With a fully distributed routing concept, higher spatial resolution in combination with the lateral transfer of water between HRUs and stream channel reaches can be considered a very important advancement in hydrological modeling toward deriving suitable conservation management scenarios.

Finally, the development and application of OMS-J2K is a significant step toward demonstrating the promise of the OMS as a viable tool for the development and maintenance of natural resource models. From the natural resources modeling viewpoint, environmental modeling frameworks such as OMS have the potential to: (1) enable easier long-term maintenance and updating of model code (the complex and convoluted code structures for most current natural resource models do not facilitate maintainability); (2) reduce duplication of work by modelers for developing common basic components, as has previously occurred with considerable duplication of code in other watershed model development efforts (e.g., SWAT, AnnAGNPS, etc.); and (3) lead to better standardization of science components over time.

Acknowledgements

We would like to thank the USDA Agricultural Research Service, the USDA Natural Resources Conservation Service, and the Departments of Civil and Environmental Engineering and Computer Science at Colorado State University for contributing to research and development of the OMS framework and associated environmental models.

References

Ahuja, L. R., J. C. Ascough II, and O. David. 2005. Developing natural resource models using the Object Modeling System: Feasibility and challenges. *Advs. Geos.* 4: 29-36.

Arnold, J. G., P. M. Allen, and G. Bernhardt. 1993. A comprehensive surface-groundwater flow model. *J. Hydrol.* 142: 47-69.

Arnold, J. G., R. Srinivasan, R. S. Muttiah, and J. R. Williams. 1998. Large-area hydrologic modeling and assessment: Part I. Model development. *J. American Water Res. Assoc.* 34(1): 73-89.

Arnold, J. G., R. S. Muttiah, R. Srinivasan, and P. M. Allen. 2000. Regional estimation of base flow and groundwater recharge in the upper Mississippi River basin. *J. Hydrol.* 227: 21-40.

Ascough II, J. C., D. C. Flanagan, O. David, and L. R. Ahuja. 2005. Assessing the potential of the Object Modeling System (OMS) for erosion prediction modeling. ASABE Paper No. 052011. St. Joseph, Mich.: ASABE.

Bosch, D. D., J. M. Sheridan, H. L. Batten, and J. G. Arnold. 2004. Evaluation of the SWAT model on a coastal plain agricultural watershed. *Trans. ASAE* 47(5): 1493-1506.

Castleton, K. J., and G. M. Gelston. 2003. FRAMES 2.x: Science to solutions multimodel operating system. PNNL Working Paper SA-39446. Richland, Wash.: Pacific Northwest National Laboratory.

Chaubey, I., C. T. Haan, J. M. Salisbury, and S. Grunwald. 1999. Quantifying model output uncertainty due to spatial variability of rainfall. *J. American Water Res. Assoc.* 35(5): 1-10.

Das, S., R. P. Rudra, P. K. Goel, R. Gharabaghi, and N. Gupta. 2006. Evaluation of AnnAGNPS in cold and temperate regions. *Water and Science Tech.* 53(2): 262-270.

David, O., S. L. Markstrom, K. W. Rojas, L. R. Ahuja, and I. W. Schneider. 2002. The Object Modeling System. In *Agricultural System Models in Field Research and Technology Transfer*, 317-330. L. R. Ahuja, L. Ma, and T. A. Howell, eds. Boca Raton, Fla.: Lewis Publishers.

David, O., J. Ascough, G. Leavesley, and L. Ahuja, 2010. Rethinking modeling framework design: Object Modeling System 3.0. In *Proc. 5th iEMSs Biennial Meeting: Modeling for Environment's Sake* (Ottawa, Ontario, Canada). D. Swayne, W. Yang, A. Voinov, A. Rizzoli, and T. Filatova, eds. Manno, Switzerland: International Environmental Modeling and Software Society.

Dickinson, R. E. 1984. Modelling evapotranspiration for three-dimensional global climate models. In *Climate Processes and Climate Sensitivity*, 58-72. Geophysical Monograph Series, Vol. 29. J. E. Hansen and T. Takahasi, eds. Washington, D.C.: American Geophysical Union.

Di Luzio, M., J. G. Arnold, and R. Srinivasan. 2005. Effects of GIS data quality on small watershed streamflow and sediment simulations. *J. Hydrol. Proc.* 19(3): 629-650.

Donigan, A. S., J. C. Imhoff, B. R. Bicknell, and J. L. Little. 1984. Application guide for Hydrological Simulation Program — Fortran (HSPF). EPA 600/3-84-065. Athens, Ga.: U.S. EPA Environmental Research Laboratory.

Duan, Q., V. K. Gupta, and S. Sorooshian. 1992. Effective and efficient global optimization for conceptual rainfall-runoff models. *Water Resour. Res.* 28(4): 1015-1031.

Duan, Q., V. K. Gupta, and S. Sorooshian. 1993. A shuffled complex evolution approach for effective and efficient global minimization. *J. Optimization Theory Appl.* 76(3): 501-521.

Duriancik, L. F., D. Bucks, J. P. Dobrowolski, T. Drewes, S. D. Eckles, L. Jolley, R. L. Kellogg, D. Lund, J. R. Makuch, M. P. O'Neill, C. A. Rewa, M. R. Walbridge, R. Parry, and M. A. Weltz. 2008. The first five years of the Conservation Effects Assessment Project. *J. Soil. Water Cons.* 63(6): 185A-197A.

Feyereisen, G. W., T. C. Strickland, D. D. Bosch, and D. G. Sullivan. 2007. Evaluation of SWAT manual calibration and input parameter sensitivity in the Little River watershed. *Trans. ASABE* 50(3): 843-855.

Fontaine, T. A., T. S. Cruickshank, J. G. Arnold, and R. H. Hotchkiss. 2002. Development of a snowfall-snowmelt routine for mountainous terrain for the soil water assessment tool (SWAT). *J. Hydrol.* 262: 209-223.

Green, W. H., and G. A. Ampt. 1911. Studies on soil physics: 1. Flow of air and water through soils. *J. Agric. Sci.* 4: 1-24.

Gregersen, J. B., P. J. A. Gijsbers, and S. J. P. Westen. 2007. OpenMI: Open modelling interface. *J. Hydroinformatics* 9(3): 175-191.

Gupta, H. V., S. Sorooshian, and P. O. Yapo. 1999. Status of automatic calibration for hydrologic models: Comparison with multilevel expert calibration. *J. Hydrologic Eng.* 4(2): 135-143.

Haan, C. T. 1989. Parametric uncertainty in hydrologic modeling. *Trans. ASAE* 32(1): 137-146.

Heathman, G. C., M. Larose, and J. C. Ascough II. 2009. Soil and Water Assessment Tool evaluation of soil and land use geographic information data sets on simulated streamflow. *J. Soil. Water Cons.* 64(1): 17-32.

Hill, C., C. DeLuca, V. Balaji, M. Suarez, and A. da Silva. 2004. The architecture of the Earth System Modeling Framework. *Comp. Sci. Eng.* 6(1): 18-28.

Hoblit, B., B. Vieux, A. Holder, and P. Bedient. 1999. Predicting with precision. *Civil Eng. Magazine* 69(11): 40-43.

IDNR. 1980. *The Indiana Water Resource (Vol. 1): Availability, Uses, and Needs*. G. D. Clark, ed. Indianapolis, Ind.: Indiana Department of Natural Resources.

IDNR. 1987. Water resource availability in the St. Joseph River basin, Indiana. J. Beaty and C. Clendenon, eds. Water Resource Assessment 87-1. Indianapolis, Ind.: Indiana Department of Natural Resources, Division of Water.

Kralisch, S., and P. Krause. 2006. JAMS: A framework for natural resource model development and application. In *Proc. 3rd iEMSs Biennial Meeting: Summit on Environmental Modelling and Software* (Burlington, Vt.). A. Voinov, A. J. Jakeman, and A. E. Rizzoli, eds. Manno, Switzerland: International Environmental Modelling and Software Society.

Krause, P. 2002. Quantifying the impact of land use changes on the water balance of large catchments using the J2000 model. *Phys. Chem. Earth* 27(9-10): 663-673.

Krause, P., U. Bende-Michl, F. Bäse, M. Fink, W-A. Flügel, and B. Pfennig. 2006. Multiscale investigations in a mesoscale catchment: Hydrological modelling in the Gera catchment. *Adv. Geos.* 9: 53-61.

Larose, M., G. C. Heathman, D. L. Norton, and B. Engle. 2007. Hydrologic and atrazine simulation in the Cedar Creek watershed using the SWAT model. *J. Environ. Qual*. 36(2): 521-531.

Manguerra, H. B., and B. A. Engel. 1998. Hydrologic parameterization of watersheds for runoff prediction using SWAT. *J. American Water Res. Assoc*. 34(5): 1149-1162.

Mausbach, M. J., and A. R. Dedrick. 2004. The length we go measuring environmental benefits of conservation practices. *J. Soil and Water Cons.* 59(5): 96-103.

Monteith, J. L. 1975a. Vol. 1: Principles. In *Vegetation and Atmosphere*. London, U.K.: Academic Press.

Monteith, J .L. 1975b. Vol. 2: Case studies. In *Vegetation and Atmosphere*. London, U.K.: Academic Press.

Moriasi, D. N., J. G. Arnold, M. W. Van Liew, R. L. Binger, R. D. Harmel, and T. L. Veith. 2007. Model evaluation guidelines for systematic quantification of accuracy in watershed simulations. *Trans. ASABE* 50(3): 885-900.

Motovilov, Y. G., L. Gottschalk, K. Engeland, and A. Rodhe. 1999. Validation of distributed hydrological model against spatial observations. *Agric. Forest Meteorol*. 98-99: 257-277.

NOAA-NCDC. 2004. Climate monitoring. Asheville, N.C.: National Oceanic and Atmospheric Administration, National Climate Data Center. Available at: www.ncdc.noaa.gov/climate-monitoring/index.php. Accessed 10 August 2011.

Parajuli, P. B., N. O. Nelson, L. D. Frees, and K. R. Mankin. 2009. Comparison of AnnAGNPS and SWAT model simulation results in USDA-CEAP agricultural watersheds in south-central Kansas. *J. Hydrol. Proc.* 23(5): 748-763.

Richardson, C. W., and D. A. Wright. 1984. WGEN: A model for generating daily weather variables. ARS-8. Washington, D.C.: USDA Agricultural Research Service.

Rizzoli, A. E., G. H. Leavesley, J. C. Ascough II, R. M. Argent, I. N. Athanasiadis, V. C. Brilhante, F. H. Claeys, O. David, M. Donatelli, P. Gijsbers, D. Havlik, A. Kassahun, P. Krause, N. W. Quinn, H. Scholten, R. S. Sojda, and F. Villa. 2008. Chapter 7: Integrated modelling frameworks for environmental assessment and decision support. In *Environmental Modelling and Software and Decision Support: Developments in Integrated Environmental Assessment (DIEA)*, 3: 101-118. A. J. Jakeman, A. A. Voinov, A. E. Rizzoli, and S. H. Chen, eds. The Netherlands: Elsevier.

Santhi, C., J. G. Arnold, J. R. Williams, W. A. Dugas, R. Srinivasan, and L. M. Hauck. 2001. Validation of the SWAT model on a large river basin with point and nonpoint sources. *J. American Water Resources Assoc.* 37(5): 1169-1188.

Sarangi, A., C. A. Cox, amicromnd C. A. Madramootoo. 2007. Evaluation of the AnnAGNPS model for prediction of runoff and sediment yields in St. Lucia watersheds. *Biosystems Eng.* 97(2): 241-256.

Scheffler, C., W.-A. Flügel, and P. Krause. 2005. Hydrological modelling for quantification of coarse scale soil moisture in southern Africa. In *MODSIM 2005 Intl. Congress on Modelling and Simulation*, 170-176. A. Zerger and R. M. Argent, eds. Canberra, Australia: Modelling and Simulation Society of Australia and New Zealand.

Spruill, C. A., S. R. Workman, and J. L. Taraba. 2000. Simulation of daily and monthly stream discharge from small watersheds using the SWAT model. *Trans. ASAE* 43(6): 1431-1439.

SJRWI. 2004. Cedar Creek watershed management plan. ARN 01-383. Fort Wayne, Ind.: St. Joseph River Watershed Initiative. Available at: www.sjrwi.org/documents/CCWMP-finaldraft 081505.pdf. Accessed 10 August 2011.

Tolson, B. A., and C. A. Shoemaker. 2007. Cannonsville reservoir watershed SWAT2000 model development, calibration and validation. *J. Hydrol.* 337(1-2): 68-86.

USDA-ARS. 2004. ARS watershed assessment study plan, National program 201: Water quality and management. Washington, D.C.: USDA Agricultural Research Service. Available at: ftp://ftp-fc.sc.egov.usda.gov/NHQ/nri/ceap/arsceapprojectplan.pdf. Accessed 10 August 2011.

USDA-NASS. 2001. USDA-NASS homepage. Washington, D.C.: USDA National Agricultural Statistics Service. Available at: www.nass.usda.gov/index.asp. Accessed 10 August 2011.

Van Liew, M. W., and J. Garbrecht. 2003. Hydrologic simulation of the Little Washita River experimental watershed using SWAT. *J. American Water Resources Assoc.* 39(2): 413-426.

Van Liew, M. W., J. G. Arnold, and D. D. Bosch. 2005. Problems and potential of autocalibrating a hydrologic model. *Trans. ASAE* 48(3): 1025-1040.

Van Liew, M. W., T. L. Veith, D. D. Bosch, and J. G. Arnold. 2007. Suitability of SWAT for the Conservation Effects Assessment Project: Comparison on USDA Agricultural Research Service watersheds. *J. Hydrol. Eng*. 12(2): 173-189.

Wang, X., and A. M. Melesse. 2006. Effects of STATSGO and SSURGO as inputs on SWAT model's snowmelt simulation. *J. American Water Resources Assoc.* 42(5): 1217-1236.

White, K. L., and I. Chaubey. 2005. Sensitivity analysis, calibration, and validation for a multisite and multivariable SWAT model. *J. American Water Resources Assoc.* 41(5): 1077-1089.

Yuan, Y., R. L. Bingner, and R. A. Rebich. 2001. Evaluation of AnnAGNPS on Mississippi Delta MSEA watersheds. *Trans. ASAE* 44(5): 1183-1190.